ISTANBUL TECHNICAL UNIVERSITY ★ GRADUATE SCHOOL OF SCIENCE
ENGINEERING AND TECHNOLOGY

CONTROL OF SEPARATION
CLUTCH SYSTEM FOR CLUTCH CLOSING

M.Sc. THESIS

Berkan KAÇMAZ

Department of Control and Automation Engineering

Control and Automation Engineering Programme

JULY 2020

ISTANBUL TECHNICAL UNIVERSITY ★ GRADUATE SCHOOL OF SCIENCE ENGINEERING AND TECHNOLOGY

CONTROL OF SEPARATION CLUTCH SYSTEM FOR CLUTCH CLOSING

M.Sc. THESIS

Berkan KAÇMAZ
(504171103)

Department of Control and Automation Engineering

Control and Automation Engineering Programme

Thesis Advisor: Prof. Dr. M. Turan SÖYLEMEZ

JULY 2020

İSTANBUL TEKNİK ÜNİVERSİTESİ ★ FEN BİLİMLERİ ENSTİTÜSÜ

DEBRIYAJ KAPATMA SIRASINDA AYIRICI DEBRIYAJ KONTROLU

YÜKSEK LİSANS TEZİ

Berkan KAÇMAZ
(504171103)

Kontrol ve Otomasyon Mühendisliği Anabilim Dalı

Kontrol ve Otomasyon Mühendisliği Programı

Tez Danışmanı: Prof. Dr. M. Turan SÖYLEMEZ

TEMMUZ 2020

Berkan KAÇMAZ, a M.Sc. student of ITU Graduate School of Science Engineering and Technology student ID 504171103 successfully defended the thesis entitled "CONTROL OF SEPARATION CLUTCH SYSTEM FOR CLUTCH CLOSING", which he/she prepared after fulfilling the requirements specified in the associated legislations, before the jury whose signatures are below.

Thesis Advisor :	**Prof. Dr. M. Turan SÖYLEMEZ** Istanbul Technical University	....
Jury Members :	**Prof. Dr. Metin GÖKAŞAN** İstanbul Technical University	....
	Prof. Dr. Alpaslan PARLAKÇI İstanbul Bilgi University	....
		....

Date of Submission : **15 June 2020**
Date of Defense : **17 July 2020**

__To my family...__

FOREWORD

I would like to express my special thanks to my graduation project advisor Prof. Dr. Mehmet Turan SÖYLEMEZ, for his contribution, interest, and guidance. I offer my endless gratitude to Esra GÜBEN, who has a significant share in my success for her constant support and inspiration. Finally, I like to thank my family for their support for all my life long.

13 JULY 2020

Berkan KAÇMAZ
(Bsc.)

TABLE OF CONTENTS

Page

ABBREVIATIONS

ECU	: Engine Control Unit
EM	: Electric Motor
HEV	: Hybrid and Electrical Vehicles
ICE	: Internal Combustion Engine
LQG	: Linear Quadratic Gaussian
LQR	: Linear Quadratic Regulator
MCU	: Motor Control Unit
MPC	: Model Predictive Control
PD	: Proportional Derivative
PI	: Proportional Integral
PID	: Proportional Integral Derivative
PInd	: Performance Index
SISO	: Single Input Single Output
TCU	: Transmission Control Unit

SYMBOLS

ω_i	: Input Shaft Speed
ω_o	: Output Shaft Speed
T_i	: Input Shaft Torque
T_o	: Output Shaft Torque
T_f	: Friction Torque
b_i	: Input Shaft Damping Ratio
b_o	: Output Shaft Damping Ratio
ω_{slip}	: Slip Speed
μ	: Viscous Drag Coefficient
k_k	: Kinetic Friction Coefficient Between Clutch Discs
D	: Clutch De-rating Factor
N_{disc}	: Number of Friction Surfaces
r_{eff}	: Effective Torque Radius
P_c	: Applied Clutch Pressure
A	: Surface Area
P_{eng}	: Engagement Pressure
u	: Control Signal/Input
e	: Error
K_p	: Proportional Gain
K_i	: Integral Gain
K_d	: Derivative Gain
Q	: Weighting Factor Matrix for State Errors
R	: Weighting Factor Matrix for Regulating
$\dot{T}_i$	: Input Torque Changes
$\dot{T}_o$	: Output Torque Changes
N_p	: Prediction Horizon
N_c	: Control Horizon
d_k	: Disturbance Measurement
w	: Processed white noise
v	: White Measurement Noise

LIST OF TABLES

Page

LIST OF FIGURES

Page

CONTROL OF SEPARATION CLUTCH SYSTEM FOR CLUTCH CLOSING

SUMMARY

Transportation is an essential subject in the modern world. For years, internal combustion engine-based vehicles dominated the industry. With advancing technologies, more and more vehicles became available to people; thus, resulted in some issues. Increasing doubt about oil supply renewability, expectations of better fuel economy and growing concerns for the environmental effect of carbon and nitrogen waste emissions resulting primarily from internal combustion engines have driven the industry to alternate approaches. Although there are several alternative ideas for these issues, hybrid electric vehicles have been focused and become more popular in the world in recent years.

Although there are several perspectives for classifying the hybrid electrical vehicles, they can be grouped into series hybrid and parallel hybrid, and more complex ones with combinations of these. In the series hybrid, the electric motor is the only torque source for driving the vehicle. In contrast, the internal combustion engine is used to charge the battery only and is not connected to wheels by a mechanical link. On the other hand, in a parallel hybrid, both engine and electric motor can be used as torque sources for vehicles. There are various configurations in terms of power structure with the opportunity of driving modes. Parallel hybrid structures can be classified depending on the electrification capabilities of the vehicle, such as micro-hybrid, mild hybrid, and full hybrid. In a general representation of parallel hybrid vehicles, there are various driving modes such as electric-only mode, internal combustion mode only, boost. Also, in parallel hybrid vehicles, there are various types of hybrid powertrain structures. One of the most common ones is the P2 hybrid vehicle, which is a parallel hybrid structure. In this type, the electric motor and internal combustion engine are separated via a separation clutch, and it is essential to control this clutch during engaging since it connects the two traction sources of the vehicle.

The thesis aims to provide a theoretical solution to the real-time practical problem, particularly for P2 hybrid vehicle systems, the separation clutch closing control. Classical control methods such as proportional-integral-derivative (PID), proportional-integral proportional-derivative PI-PD, optimal control methods such as linear quadratic regulator (LQR), LQR with known disturbances, and model predictive control methods are applied for control of the system.

Initially, the mathematical system model is examined, and the state-space model is determined by separating the system from other parts (e.g., engine and electric motor) of the powertrain and considering it as a single unit. Then, a classical PID controller is used for control of the system. After that, a PI-PD controller, which is a more

sophisticated method, is used in the system to solve the overshoot issue and provide more comprehensive control possibilities using the PI-PD due to its advantages over PID. By analyzing the results, it is deduced that the performance of PI-PD controller is better over classical PID in terms of overshoot in system response.

A state-space model empowers the controller designer to use optimal control methods. So, control of the system is performed via an LQR controller, which has a static controller structure. The disturbances (input and output torque changes) for the system can be measured via sensors or calculated by other control units. Thus, considering disturbances as known features for the system, LQR with known disturbances structure is used for control of the system. The LQR with known disturbances outperformed the classical LQR considering system response with the additional information. Additionally, LQR with known disturbance is relatively robust according to simulations with the dynamic system model during operation.

After that, a classical MPC controller is designed for a nominal system with known disturbances structure similar to the LQR approach. The multi-MPC structure is also implemented for control of the system for dynamic model changes during operation since the MPC algorithm highly depends on the accuracy of the model. For providing a more realistic approach, system feedback information is obtained from a Kalman filter.

The system responses with PI-PD controller, LQR with known disturbances, and multi-MPC structures are compared in terms of the determined performance index and controller cost. LQR and MPC structures are implemented with Kalman filter in simulations. PI-PD can only control the slip speed due to the single input-single output control structure, which makes it harder to control two outputs of the system. Hence it has the worst system response in terms of the performance index. The system with the Multi-MPC controller has the best result considering the performance index while LQR with known disturbances, whereas the LQR controller performance, is between these two methods.

Considering the separation clutch system as a compact unit is one of the benefits of this study. Most control approaches of clutch closing algorithms try to control other elements in powertrain together. Unlike most studies and applications in the industry, the system in this study is considered as independent from other elements of the powertrain system, such as electric motor, engine, and transmission in control perspective.

The solution for controlling the system is provided with different control methods using classical and more sophisticated structures. Moreover, the real-time aspects of the system, such as feedback for the controller and dynamic model changes during operation, are also considered for simulating the controllers to provide more suitable solutions for practical problems.

DEBRIYAJ KAPATMA SIRASINDA AYIRICI DEBRIYAJ KONTROLU

ÖZET

Ulaşım, modern dünya için önemli bir konudur. Yıllardır, içten yanmalı motorlu araçlar sektöre hakim olmuştur. Gelişen teknolojiler sayesinde giderek daha fazla araç insanlar tarafından kullanılabilir hale geldi. Bunun sonucu olarak bazı problemler de ortaya çıktı. Petrol arzının yenilenebilirliği konusunda artan şüphe, daha iyi yakıt ekonomisi beklentileri ve özellikle içten yanmalı motorlardan kaynaklanan karbon ve azot atığı emisyonlarının çevresel etkileri konusunda artan endişeler, otomotiv sektörünün alternatif yaklaşımlara yönelmesine sebep olmuştur. Her ne kadar bu konuları çözmek için farklı birçok alternatif fikir bulunmuş ve çalışılmış olsa da, hibrit elektrikli araçlara odaklanıldı. Böylece hibrit araçlar son yıllarda dünyada daha popüler hale geldi.

Hibrit elektrikli araçların sınıflandırılması için birçok perspektif olmasına rağmen, bunlar seri hibrit, paralel hibrit ve bunların kombinasyonları ile anlatılabilecek daha karmaşık olanlar olarak gruplandırılabilir. Seri hibrit araçlarda elektrik motor, aracı sürmek için tek tork kaynağı iken içten yanmalı motor yalnızca bataryayı şarj etmek için kullanılır ve mekanik bir bağlantı ile tekerleklere bağlanmaz. Öte yandan, paralel hibrit araçlarda, hem içten yanmalı motor hem de elektrik motoru araç için tork kaynağı olarak kullanılabilir. Bununla birlikte çeşitli güç aktarma organı yapılandırmaları ile farklı sürüş modlarına olanak tanınmış olur. Paralel hibrit araçlar, aracın elektrifikasyon özelliklerine bağlı olarak mikro hibrit, hafif hibrit ve tam hibrit gibi sınıflandırılabilir. Genel olarak paralel hibrit araçlarda, sadece elektrikli mod, sadece içten yanmalı mod, takviye modu gibi çeşitli sürüş modları vardır. Ayrıca bu araçlarda çeşitli hibrit güç aktarma yapılandırmaları vardır. En yaygın olanlardan biri, paralel bir hibrit yapı olan P2 hibrit aracıdır. Bu tipte, elektrik motoru ve içten yanmalı motor bir ayırma kavraması ile ayrılır ve aracın iki çekiş kaynağını bağladığı için kavrama sırasında bu kavramanın kontrol edilmesi önemlidir.

Bu tez çalışmasında, gerçek zamanlı pratik bir problem olan P2 tipi hibrit araç sistemlerinde elektrik motor ve içten yanmalı motor arasında bulunan ayırıcı debriyaj sisteminin kapatma kontrolüne teorik bir çözüm sunmak amaçlanmıştır. Yapılan çalışmada, ayırıcı debriyaj sisteminin kapatma sırasındaki kontrolü için öncelikle birer klasik kontrol yöntemi olan oransal-integral-türevsel denetleyici (PID) ve oransal-integral oransal-türevsel denetleyici (PI-PD) kontrol yapıları kullanılmıştır. Bundan sonra, bir optimal kontrol yöntemi olan standart yapıdaki doğrusal kuadratik regülatör (LQR) ve daha sonrasında bu yönteme ek olarak ölçülebilir bozucu yapısına sahip LQR kullanılmıştır. Son olarak, sisteme farklı bir optimal kontrol yöntemi olan model öngörülü kontrolcü yapısı da uygulanmıştır.

İlk olarak, ayırıcı debriyaj sistemi araçtaki diğer güç aktarma organlarından (örneğin içten yanmalı motor ve elektrik motoru) ayrı bir ünite olarak düşünülmüştür. Daha sonra bu fiziksel sistemin matematik sistem modeli incelenmiş ve durum-uzay modeli elde edilmiştir. Ardından, sistem durum uzay modelinden elde edilen transfer fonksiyonu kullanılarak klasik bir PID kontrolörü ile kontrol edilmiştir. Sonrasında, PID kontrol kullanılmış sistem cevabı sonuçlarında ortaya çıkan aşım sorununu çözmek ve daha kapsamlı kontrol olanakları sağlamak için PID yöntemine göre farklı avantajları olan ve daha gelişmiş bir kontrol yapısına sahip olan PI-PD kontrolör, sistemin kontrolü için kullanılmıştır. Sistem cevapları analiz edildiğinde PI-PD kontrolörün klasik PID'ye göre aşım problemlerini çözmede daha başarılı olduğu gözlemlenmiştir.

Bir fiziksel sistem kontrolü için sistemin durum-uzay matematiksel modeline sahip olmak, kontrolör tasarımcısına optimal kontrol yöntemlerini kullanabilme olanağı tanır. Bu sebeple, sistemin kontrolü, statik bir kontrolör yapısına sahip olan LQR kontrol ile gerçekleştirilmiştir. Sistemin matematik modeline göre ilk başta bozucu olarak kabul edilen sinyaller (giriş şaftındaki tork değişimi ve çıkış şaftındaki tork değişimi), aslında sensörler üzerinden ölçülebilir veya diğer kontrol üniteleri tarafından hesaplanabilir. Bu sebeple, klasik LQR yapısından hareket ile bu bozucu sinyaller sistem için ölçülebilir bozucular olarak kabul edilerek ölçülebilir bozucu yapısına sahip LQR kontrolörü sistem için kullanılmıştır. Ölçülebilir bozucu yapısına sahip LQR, kullandığı bozucu sinyal bilgileriyle klasik LQR ile kontrol edilen sisteme kıyasla daha iyi sonuçlar göstermiştir. Diğer bir deyişle ölçülebilir bozucu yapısına sahip LQR, klasik LQR yapısından daha iyi performans göstermiştir. Ayrıca, benzetim sonuçlarına göre ölçülebilir bozucu yapısına sahip LQR'ın çok büyük dinamik sistem modeli değişikleri olmadıkça dayanıklı bir yapıya sahip olduğu da gözlemlenmiştir.

Daha sonra, sistemin kontrolü için klasik bir model öngörülü kontrolcü, LQR yöntemindekine benzer bir şekilde, ölçülebilir bozucu yapısına sahip olarak tasarlanmıştır. Ayırıcı debriyaj sisteminde çalışma sırasında sistemin parametreleri dinamik olarak değiştiğinden sistemin matematiksel modelinin de değiştiği göz önünde bulundurulmuştur. Model öngörülü kontrolcü algoritması büyük ölçüde matematiksel modelin fiziksel sistemi doğru bir şekilde ifade etmesine bağlıdır. Bu yüzden bu sistem dinamiklerine karşı daha gelişmiş bir yapı olan çoklu model öngörülü kontrolcü yapısı dinamik sistemin kontrolü için de uygulanmıştır. Buna ek olarak, sistemde bir Kalman filtresi uygulanmıştır. Buradaki amaç, gerçek sistem dinamiklerine karşı daha uygun bir yaklaşım sağlayarak sistem geri bildirimini bu filtreden elde etmektir.

Son olarak, sistemin kontrolü için kullanılan yapılardan PI-PD kontrolörü, ölçülebilir bozucu yapısına sahip LQR ve çoklu model öngörülü kontrolcü yapılarına sahip sistem yanıtları karşılaştırılarak bu yöntemler arasında bir değerlendirme yapılmıştır. Kontrol yöntemlerinin karşılaştırılması için sistem yanıtlarına bağlı hesaplanan bir performans endeksi ve kontrolcü çıktılarına bağlı hesaplanan bir kontrolör maliyeti göz önünde bulundurulmuştur. Ölçülebilir bozucu yapısına sahip LQR ve çoklu model öngörülü kontrolcü yapılarının benzetimleri için sistemin gerçek dinamik özelliklerine karşı bir çözüm olarak sunulan Kalman filtresi kullanılmıştır. PI-PD kontrolcü, tek giriş-tek çıkış kontrol yapısına sahip olması sebebiyle sadece kayma hızını kontrol edebilir; bu da sistemin iki çıkışını kontrol etmeyi zorlaştırır. Dolayısıyla, performans endeksi açısından en kötü sistem yanıtına PI-PD sistem cevabı sahiptir. Çoklu model öngörülü kontrolöre sahip sistem sonucu performans endeksi dikkate alındığında en iyi sonuca sahipken, ölçülebilir bozucu yapısına sahip LQR'ın kullanıldığı sistem sonucu performansı değeri diğer iki yöntem arasında elde edilmiştir.

Ayırıcı debriyaj sistemini kompakt bir ünite olarak ele alarak araçtaki diğer güç aktarım organlarından bağımsız olarak analiz etmek bu çalışmanın faydalarından biridir. Ayırıcı debriyaj kapatma algoritmalarının çoğu, güç aktarım sistemlerindeki diğer elemanları birlikte kontrol etmeye çalışır. Endüstride yapılan çoğu çalışma ve uygulamanın aksine, bu çalışmadaki sistem, elektrik motoru, içten yanmalı motor ve şanzıman gibi güç aktarma sisteminin diğer elemanlarından bağımsız olarak kabul edilmiştir. Bu diğer yapıların etkileri de incelenen sistem için birer bozucu olarak kabul edilmiştir.

Sistemin kontrolüne yönelik çözüm için önce klasik sonra da daha karmaşık yapılar kullanılarak farklı kontrol yöntemleri ele alınmıştır. Ayrıca, kontrolörler için geri bildirim mekanizması için gerçek zamanlı sistemin geri bildirimi sırasındaki kısıtlamalar ve sitemin çalışması sırasında oluşan dinamik model değişiklikleri de göz önüne alınarak farklı yapılar düşünülmüştür. Böylece kullanılan yöntemlerde, benzetim yapılırken gerçek zamanlı sistemde oluşabilecek problemler için daha uygun çözümler oraya konulmaya çalışılmıştır.

1. INTRODUCTION

1.1 Introduction and Aim of Thesis

In recent years, electric motors are preferred to be used together with internal combustion engines in the vehicle industry. As a result, usage and investment on hybrid vehicles are increased due to their advantages over vehicles with petrol-based engines in terms of fuel consumption, overall efficiency, and overall carbon oxides (CO, CO_2) emissions. However, their nontraditional powertrain structures make the production of hybrid vehicles a challenging task for the suppliers in terms of control and calibration processes.

There are several structures in hybrid vehicles, such as serial, parallel, and power split. One of the parallel structures in parallel hybrid structures is P2 type, which has two torque sources (engine and electric motor) in the same shaft before transmission and separated with a separation clutch [2]. One of the challenging problems in this structure is controlling the clutch closing sequence/process of the separation clutch between the engine and the electric motor in parallel hybrid vehicles.

Although the control of the hybrid system components such as the engine, e-motor, and transmission are well studied in the literature [8–11], the studies focusing particularly on separation clutch control are not very common. In industry, the control of different hybrid components is performed by separate control units (e.g., engine control unit (ECU), motor control unit (MCU), transmission control unit (TCU)). This has many advantages such as better management of work split for manufacturers, buying the components as modular packages with dedicated control software, and keeping the teams separate for development.

Separating development teams is an essential aspect of automotive since it increases the effectiveness of the distribution of specialists in particular areas. Additionally, it enables manufacturers to be able to hire different companies for software support.

Although the control of this system might be embedded into one control unit rather than have a separate module, the control of the system is separated as a concept. In industry, it is managed by rule-based control algorithms or algorithms together with classical concepts (e.g., reference tracking [12, 13]) and the calibration of these algorithms for use cases determined for the application in particular vehicle structures [14, 15].

Thus, this paper aims to provide a theoretical solution for a practical problem, namely control of the separation clutch closing process, by considering the application of the control unit's modularity. To this end, the process is decided to controlled by using the well-known classical and more advanced control theories for implementing only with system inputs and outputs.

First, the physical model of the separation clutch system during slipping is examined for finding a mathematical model for using the control theories. Then, the system is controlled by well-studied control methods such as PID, LQR, and MPC. Moreover, some further developments (PIPD, LQR with known disturbances, and Multi-MPC) are implemented to control the system more efficiently and make the structures more suitable for real-time applications. After that, the results are compared in terms of performance and control cost.

2. HYBRID VEHICLES AND POWERTRAIN STRUCTURE

2.1 Hybrid Vehicle Structure

Transportation technologies have great importance in the world these days. Internal combustion engines are used as torque sources for the road vehicles for most of the time [16]. The fuel types for the internal combustion engines are primarily are based on oil products such as gasoline, diesel, and natural gases. However, due to the concerns regarding oil supply renewability, fuel economy, and the environmental problems based on emissions of carbon and nitrogen combustion waste, the vehicle industry is focused on alternative approaches such as hybrid electric vehicles (HEV) in recent years [1, 17, 18].

There are numerous types of hybrid electric vehicles in terms of powertrain structure. In HEVs, the internal combustion engine (ICE) and electric motor/generator (EM) are used as torque sources in different configurations. There might be different approaches for naming these structures/configurations in the industry, but generically, they can be grouped as series hybrid and parallel hybrid [19].In a series hybrid, the ICE is used as a generator for extending the driving range in the system. The torque from ICE is used only to generate electricity to the battery, not used to drive the vehicle itself [19]. While series hybrid vehicle system is more comfortable to control and capable of capturing electricity during braking or slowing down, there are some disadvantages in production since it should include a large battery pack and additional generator in the system only for ICE part [19,20]. In a parallel hybrid, both engine and motor can be used as traction sources for providing torque to the wheel to drive the vehicle [21]. In a parallel hybrid, the ICE and EM can be used in different configurations in different hybrid modes [19]:

- Electric motor can be used for regenerative braking for charging the battery

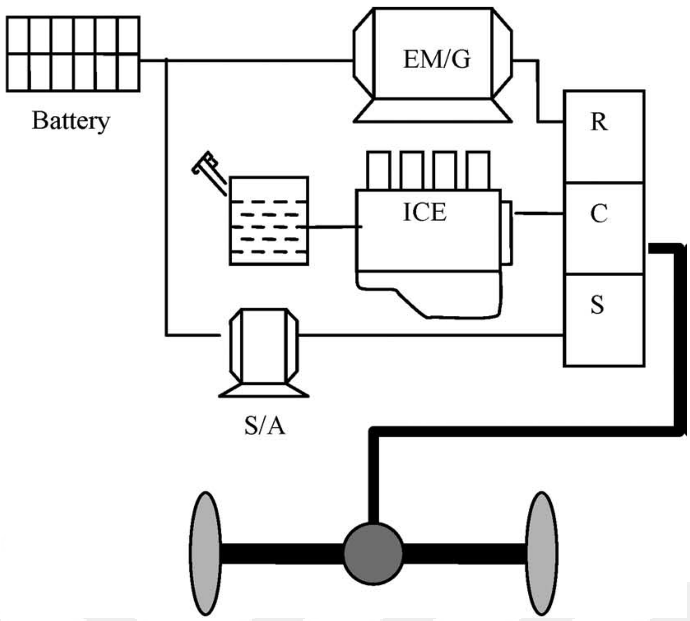

Figure 2.1: General representation of hybrid vehicle powertrain [1].

- Only EM or only ICE can be used for traction source for the vehicle (EM only & ICE only modes)
- Both EM and ICE can be used for driving the vehicle (Boost mode)
- ICE can be used for driving and charging at the same time while EM is acting as a generator in the system

In all these applications or while the operation modes are changing, it is essential to be able to split these two sources from each other with clutches [22]. Another common HEVs structure type is a series-parallel hybrid that joins together the aspects of both series and parallel hybrid HEVs by adding a new mechanical link for a series hybrid approach and adding a new generator compared to the parallel hybrid [19]. In this type, both series path and parallel path can be used with both EM and ICE. Therefore it brings opportunities for more complex but elaborative control strategies [23].

In terms of electrification of the vehicle (or other words, the function of EM), the parallel HEVs, can be classified into different groups, as in Fig.2.2. Although the classification is also depending on the exact power, voltage capabilities of electric motors and efficiency of the vehicles, the descriptions may not match the products in the industry due to different approaches by companies through years and different classification conditions by the studies. Therefore, in this study, the descriptions are given in a way for more fundamental understanding without the vehicle/electric motor's exact properties by analyzing [2, 19]. Micro hybrid is the most essential and economical type where the electric motor can only provide a small torque. The EM is essentially a starter/alternator in the vehicle responsible for the stop-start function. Mild hybrid is the next step in electrification, which provides an electric motor with more torque capabilities. The EM is responsible for assisting the ICE during driving additional to stop-start functions and even capable of regenerative braking. Compared to mild HEVs, the full (strong) hybrid vehicles have an electric motor that can generate enough traction to drive the vehicle on its own additional to mild HEVs capabilities. Together with these classifications, there are numerous structures defined for parallel HEVs according to powertrain positioning of the hybrid components. Different

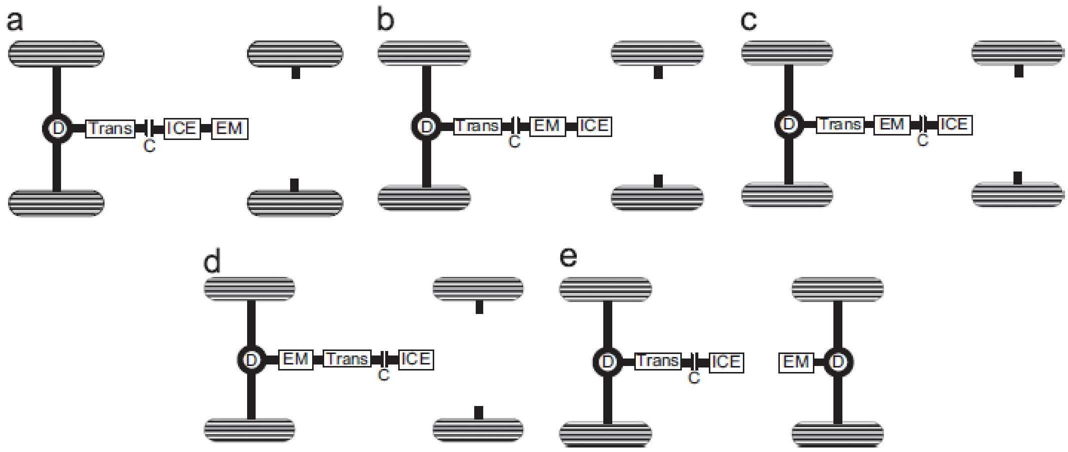

Figure 2.2: Parallel hybrid vehicle powertrain structures [2].

positioning of the components is limiting or enabling the HEVs to perform some capabilities. For example, the type-a and type-b, only EM hybrid mode (electric drive), are not possible, whereas, in the following types, EM can be separated from ICE and drive the vehicle. Also, in type-e, the torque sources are entirely separated, and they are not in the same shaft. Thus, the structure allows for more functional capabilities. In this study, the type-c parallel HEVs structure (P2 HEVs) is focused on in which the ICE and EM are connected through a clutch. This clutch is called a "separation clutch" in the industry. In industry, the clutch closing sequence is controlled by rule-based algorithms which are generally implemented via lookup tables, rule-based on/off conditions are torque/pressure requests [1].

3. MODELING AND CONTROL APPROACH OF THE CLUTCH

3.1 Mathematical Model

The separation clutch connects two torque sources in the system which are ICE and EM. In general, the control of the vehicle is separated into parts for separating the tasks and handling vehicle software implementation. Thus, the hybrid control unit (HCU) is controlling these two components. The torque requests and operating modes are determined by HCU software. Then, the engine control unit (ECU) and motor control unit (MCU) is responsible for providing these torque requests. Therefore, in this study, the internal behavior of the components is left out of scope. Then, the separation clutch model is simplified as 2 inertia/ masses connected with 2 friction plates. In both base/input and follower/output shaft, there is a torque source represented with inertia and torque. The clutch model used for this study couples the rotary input and output shafts through an idealized friction model.

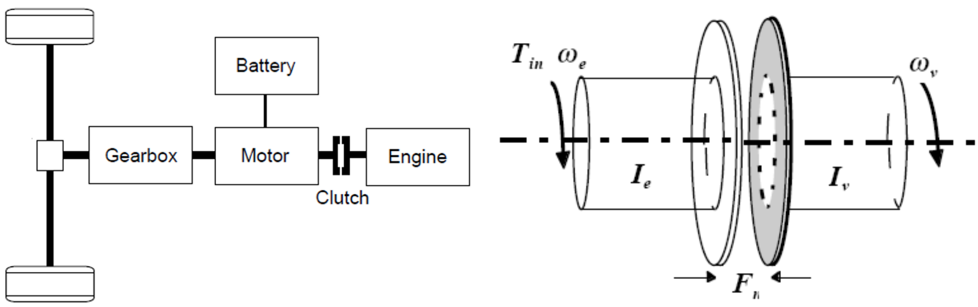

Figure 3.1: Classical friction clutch model representation [3, 4].

The clutch has three operation modes in reality which are “open”, “closed (or engaged)” and “slip (unlocked)”. The open status is generally described when there is no torque transfer between 2 plates and friction surfaces are not touching to each other, so the clutch is not operating. The closed (or engaged) status when the plates are coupled and the torque from the input shaft to the output shaft is transferred with the constraint that the clutch torque is smaller than static friction torque [24]. In slip (or unlocked) state, the system has two degrees of freedom while the friction plate speeds are different and rub each other (slipping). The power is lost as the amount of the product of kinetic friction torque and slip speed velocity [25].

In the closed (engaged) state, the clutch plates stuck to each other and they are turning in the same speed $\omega_i = \omega_o$ and there is no loss due to kinetic frictions. So, the torque transfer is provided by static friction torque and the model can be written as:

$$\dot{\omega}_i(J_o + J_i) = T_o - \omega_i(b_i + b_o) + T_i \tag{3.1}$$

Since the aim is to control the clutch during the closing process, the slip state of the clutch is considered only. In slipping, two rotational degrees of freedom are separated as shown in Fig.3.1. The friction torque is acting as a negative effect for input shaft whereas it acts as a positive effect in output shaft (input and output can be vise-versa since the clutch is bidirectional). Thus the equations of motion are as follows where ω_i is input shaft speed,ω_o is output shaft speed, T_i and T_o are input and output shaft torques, T_f is friction torque and b_i and b_o are input and output shaft damping ratios [26].

$$\dot{\omega}_i J_i = T_i - T_f + \omega_i b_i \tag{3.2}$$

$$\dot{\omega}_o J_o = T_o + T_f + \omega_o b_o \tag{3.3}$$

The difference between input and output shaft speeds is defined as slip speed (ω_{slip}). The friction torque is calculated based on viscous drag coefficient(μ), the kinetic friction coefficient between clutch discs (k_k) which is a function of ω_{slip}, the clutch de-rating the factor which accounts clutch wear (D), the number of friction surfaces (N_{disc}), the effective torque radius (r_{eff}), the applied clutch pressure (P_c), and the surface area (A), the engagement pressure (P_{eng}). If applied clutch pressure is above engagement pressure, the clutch becomes engaged. The coefficients for the nominal system is given as in Table 3.1. The friction torque is calculated as in equation 3.4 and rewritten as in equation 3.5 by combining constant variables in C_0 [4].

$$\begin{aligned} T_f &= \mu \omega_{slip} + N_{disc} P_c r_{eff} A k_k D \\ P_c &= max(P_c - P_{engd}, 0) \end{aligned} \tag{3.4}$$

$$T_f = \mu \omega_{slip} + C_0 P_c \tag{3.5}$$

Table 3.1: System parameters.

Parameter	Value
k_k	0.3
D	1
N_{disc}	2
r_{eff}	130
A	0.001
J_i	0.25
J_o	0.1

The viscous damping in input and output shafts (b_i and b_o) are considered as zero since shafts are considered as **rigid.**

With the aim of smooth torque transfer between plates, it is expected that the jerking feeling over driver will reduce and driving efficiency will be increased. Then the ω_{slip} and $\dot{\omega}_{slip}$ are decided to be controlled. Therefore, some manipulations in equations of motion are needed.

3.1.1 State space model form

The derivative of equation 3.2 and 3.3 are taken and the first equation is multiplied with J_o while the second one is multiplied with J_i. Then, the resulting first equation is subtracted from the second equation then result can be seen below.

$$J_oJ_i(\ddot{\omega}_o - \ddot{\omega}_i) = -\dot{T}_iJ_o + \dot{T}_oJ_i + (J_i + J_o)\mu(\dot{\omega}_o - \dot{\omega}_i) + (J_i + J_o)C_0\dot{P} \tag{3.6}$$

Then, the equation 3.6 is divided by J_iJ_0, the term $\frac{J_i+J_o}{J_iJ_o}$ is replaced with J_{eq}. Also, at this point, $\omega_o - \omega_i = \omega_{slip}$ is determined as a state x_1, and the derivative of slip speed ($\dot{\omega}_{slip} = \dot{\omega}_o - \dot{\omega}_i$) is determined as a state x_2. Thus, $\dot{x_2}$ is the second derivative of slip speed (($\ddot{\omega}_{slip} = (\ddot{\omega}_o - \ddot{\omega}_i$)). After that, the state-space model of the system can be written in Equation 3.7.

$$\begin{bmatrix} \dot{x_1} \\ \dot{x_2} \end{bmatrix} = \begin{bmatrix} 0 & 1 \\ J_{eq}\mu & 0 \end{bmatrix} \begin{bmatrix} x_1 \\ x_2 \end{bmatrix} + \begin{bmatrix} 0 \\ J_{eq}C_0 \end{bmatrix} \dot{P} + \begin{bmatrix} 0 & -\frac{1}{J_i} \\ \frac{1}{J_o} & 0 \end{bmatrix} \begin{bmatrix} \dot{T}_i \\ \dot{T}_o \end{bmatrix} \tag{3.7}$$

In this model, input and output torque effects are considered as disturbances. Also, it should be considered that the kinetic friction coefficient between clutch discs is a function of ω_{slip}. [4,27]. So, in simulations, the parameter C_0 can be considered as a non-linear feature of the system.

3.1.2 Controllability and observability analysis

In early examinations of system, if only the input torque is given to the system without control, the system becomes unstable as expected since this means in reality only engine torque is available and the clutch is not connected. Thus, the input shaft will speed up whereas the output shaft will not move, and the slip speed will increase. Furthermore, the system is examined and seen that it's observable and controllable.

First, the system is studied for better understanding in terms of controllability and observability. If a system can be transferred from an initial state $x(t_0)$ to a particular final state in a finite time with the input of unconstrained control vector, that system is described as controllable at time t_0 [28]. The controllability of the system can be investigated using the controllability matrix below. The system is controllable if only if the rank of the matrix has full rank [29].

$$rank\left(\left[B\ AB\ A^2B\ \ldots\ A^{n-1}B\right]\right) = n \tag{3.8}$$

If the determination of the output of a system is possible over finite time using the information initial state $x(t_0)$, the system is described to be observable at time t_0 [28].

Similarly with controllability, the observability of the system can be checked by calculating the rank of the observability matrix. The system is observable if the rank of the matrix has full rank as described in the below equation [29].

$$rank\left(\begin{bmatrix} C \\ CA \\ CA^2 \\ \vdots \\ CA^{n-1} \end{bmatrix}\right) = n \tag{3.9}$$

The system is both controllable and observable as calculated. Therefore it has been seen that using well-studied classical control methods are applicable to the system.

3.2 Control Strategies

As explained in chapter 2, the hybrid vehicle structures consist of various components to control and manage during driving. Therefore, the industry has several approaches to control the system. The approaches may depend on purely the experience in the field, control theory, computational results, or the combination of these features. The approaches can be combined into 2 main classes and those can be separated into 2 more groups. The first strategy group is based on rules while the second group of strategies is based on optimizations. Thus the two main strategy approaches can be classified as rule-based and optimization-based methods as can be seen from the Fig.3.2 . The details will be explained throughout this section.

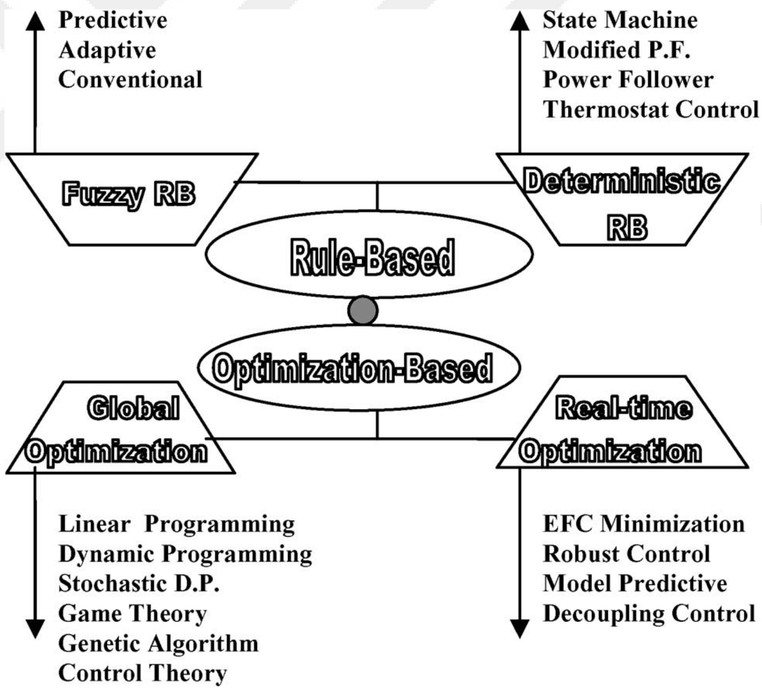

Figure 3.2: Control Strategies in hybrid vehicle controls [1].

The rule-based methods are primarily based on the rules defined based on intuition, heuristics, expert knowledge, or even mathematical models of the systems. They can be grouped into deterministic rule-based methods and fuzzy rule-based methods [1]. The modeling of most of the real systems is not a correct representation for all cycles due to non-linearity. Also, rule-based development is beneficial and easy to follow and debug in real-time applications since the rules are determined for each necessary case. Thus, rule-based approaches are quite crucial in the field.

In deterministic rule-based methods, the rules are generally determined by human expertise. This knowledge is based on the analysis of particular hybrid power-train by experts, the efficiency and limitation map from providers for components, performance goals for the vehicle such as driving comfort, emissions, and sustainability of the hybrid components (e.g., clutches, engine, electric motor). After the rules are determined, the control algorithm is generally implemented via software using deterministic calculations, look-up tables, or even classical control approaches such as (PI, PID) controllers. Then, the controller outputs are calculated using these deterministic calculations and feedbacks from the system.

Additional to deterministic rules, fuzzy rule-based methods can be considered as a reasonable approach for decision making since the hybrid drive-train has various nonlinear elements such as time-varying plants, dependencies between hybrid components. The fuzzy rules have two main advantages such as robustness (rules have tolerance for the imprecision of the measurements and variations of the hybrid components) and adaptation (the rules of fuzzy logic can be tuned easily according to necessity) [1].

The second main classification of hybrid control strategies is optimization-based methods. In this approach, generally, optimal references are determined and tried to be followed by vehicles in real-time. The references are calculated by minimizing pre-determined cost functions based on similar aspects described for deterministic methods. These methods can also be split into two main categories, such as global optimization methods and real-time optimization.

Global optimization methods try to calculate the optimal performance targets using a fixed cycle by evaluating future and past demands from vehicle and driver. Since the cycle is fixed, the calculation will not work if the nature of the cycle or conditions changes. Also, the computational effort will be much since the calculation is over the whole cycle, and algorithms aim to find the global optimal point (all possible causes should be checked). Thus this approach is not applicable for real-time applications but still a proper analysis result against real-time approaches [1].

On the other hand, the real-time optimization methods aim to find the optimal references in that exact moment and do not need to evaluate the whole cycle. The optimization calculation is instantaneous, and the algorithm tries to find the optimal control references by using optimization algorithms and current measurements from the vehicle. Although these methods are capable of working in real-time applications, the methods may still require a high computational effort than classical control methods. They may need a close representation of the physical system in the mathematical model (e.g., MPC), or the designing process may require more investment (e.g., robust) [1].

All the classification above is in terms of approaches to control strategies specifically for hybrid vehicles. Perhaps, the general picture should also be combined with generic control theory. In control theory, separation can also be made as model-based methods and rule-based methods. However, this is not directly applicable to hybrid control strategies. Model-based control can cover some applications in deterministic rule-based methods such as classical control methods (e.g., PID) and optimal control methods (e.g., LQR, LQG). These controls depend on the existence of a proper mathematical model mostly to be designed generally. Also, model-based control is applicable for real-time optimization methods such as model predictive control which highly depends on the mathematical model accuracy in real life.

The classifications described in this section are for simplifying the understanding of the concept. Similarly with "model-based methods," the direct classification might not be possible for some cases or a different categorization can be done considering different standpoint/perspective.

In industry, control of the system is mostly performed by deterministic rule-based control based on experience in the field by engineers. This control primarily depends on open-loop control of the system via determined control signals by experiments/tests and calibration of the control signal in the vehicle by fine-tuning. In this study, the mathematical model of the system is determined with the aim of using a model-based approach to control the system.

4. CONTROL of the SEPARATION CLUTCH SYSTEM

In the physical model, the main objective of the closing process of the clutch is to synchronize the input and output shaft speeds, in other words, making slip speed zero. In this study, using the state-space model, the slip speed and slip speed change rate is tried to set to zero simultaneously considering $\dot{\omega}_{slip}$ is the main effective aspect on jerk during the clutch closing phase. Firstly, for simulating the control structure with measured disturbances, the model is reconstructed in equation 4.1.

$$\begin{bmatrix} \dot{x}_1 \\ \dot{x}_2 \end{bmatrix} = \begin{bmatrix} 0 & 0 & 0 \\ J_{eq}C_0 & \frac{-1}{J_i} & \frac{-1}{J_o} \end{bmatrix} \begin{bmatrix} \dot{P} \\ \dot{T}_i \\ \dot{T}_o \end{bmatrix} \tag{4.1}$$

where the matrix B is reshaped as $\tilde{B}$ for using all system inputs together in calculations. General representation of the controller with the system in MATLAB /Simulink is given in figure 4.1.

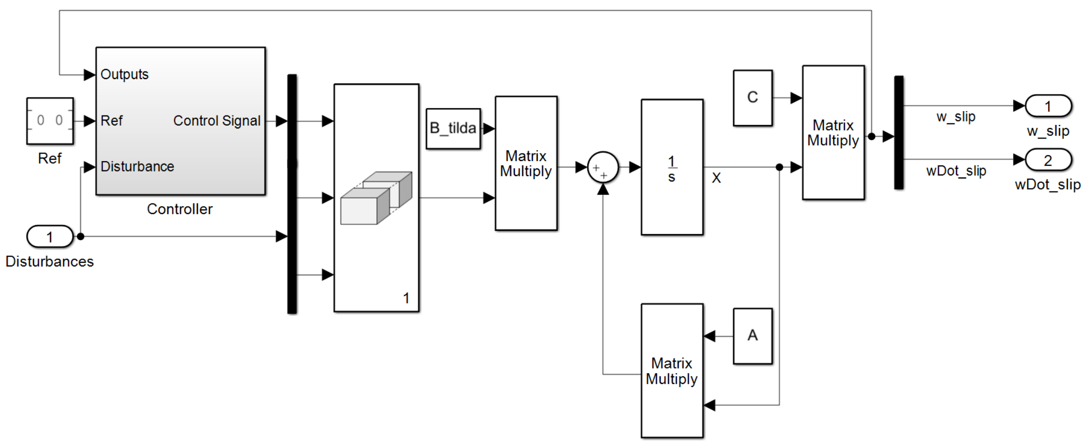

Figure 4.1: Simulink structure of the system for simulations.

4.1 Classical Control Methods: PID, PI-PD

Since the system's mathematical model enables us to use a theoretical model-based control method, the well-known classical models can be used for controlling the system. PID controller is still one of the most common control methods in the industry. The reasons are its simplicity, effectiveness over different systems under a wide range of operating conditions, and its control signal calculation algorithm which can be realized by engineers with current computer technologies [30]. It calculates the control input for the system by checking the error in the system, the change in the error and the sum (integral) in error throughout the application.

4.1.1 PID

Proportional integral derivative (PID) controllers and the modified versions of it constitute a large part of the control methods in the industry [5]. The main reasons for this are the simple and clear structure, adequate robustness, numerous tuning methods of the controller, and is one of the most widely studied methods in literature [31]. Therefore, PID control algorithms have a wide range of application areas such as process control, motor drives, magnetic and optic memories, automotive, flight control, instrumentation, etc. [32].

PID structure consists of 3 main aspects as described in the name: proportional, integral, and derivative as it is shown in Fig.4.2 below. Mainly, the controller aims to provide a control signal depending on the error in the system which is calculated as the difference between the reference and the actual system response.

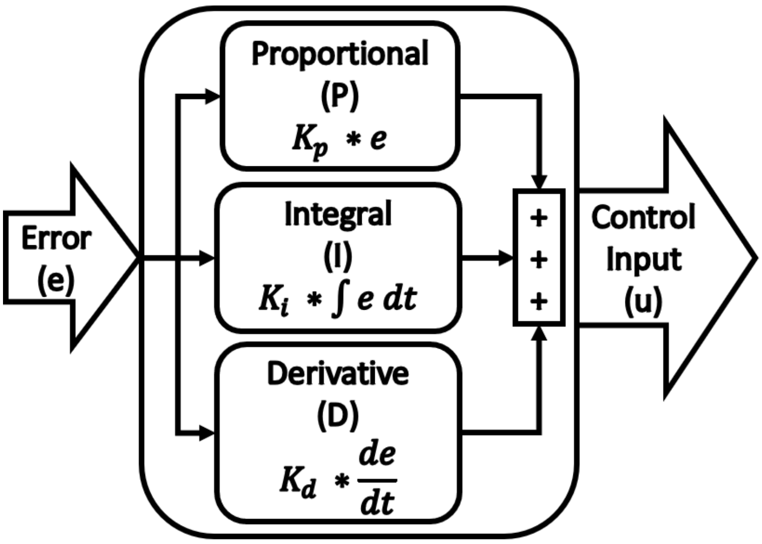

Figure 4.2: PID controller representation.

Calculating the control signal (u), the algorithm adds up the error (e) dependent controller aspects, so the controller equations can be written as below where K_p, K_i and K_d are the proportional, integral and derivative gains for the controller, respectively [33].

$$U(s) = C(s)E(s) \tag{4.2}$$

$$C(s) = K_p + K_i \frac{1}{s} + K_d s \tag{4.3}$$

There are many analytical and optimal methods for calculating the controller gains in literature such as pole-placement [34], Nyquist plot approach [35], and stability range determination for the gains [33]. The further investigation over PID gain determination is out of the scope of the study.

For using PID, the single input single output (SISO) system transfer function is calculated by choosing ω_{slip} as output and considering input and output torques as disturbances in Equation 4.4.

$$TF_{\dot{P}2\omega_{slip}} = \frac{1.092}{(s^2 - 4.44110^{-16}s - 2.8)} \tag{4.4}$$

After that, a classical PID structure is implemented, and the system is simulated with controller activation after 1.5 seconds.

The mathematical model of the system is only valid when the ω_{slip} is different from zero. If the ω_{slip} is zero, then the system is engaged, and other parts of the partial model should be used. Therefore, once the ω_{slip} is zero, the control of the system is finalized according to the current approach in this study through clutch closing control. Thus, the results are re-shaped by setting the ω_{slip} and $\dot{\omega}_{slip}$ to zero after the synchronization is completed to prevent confusions. This method is applied to a comparison of the results throughout the paper.

4.1.2 PI-PD

As it can be seen from Fig.4.3 that the system has an overshoot. For solving this problem, a further complex method, Proportional integral- proportional derivative (PI-PD) structure is recommended because it has satisfactory results in the literature

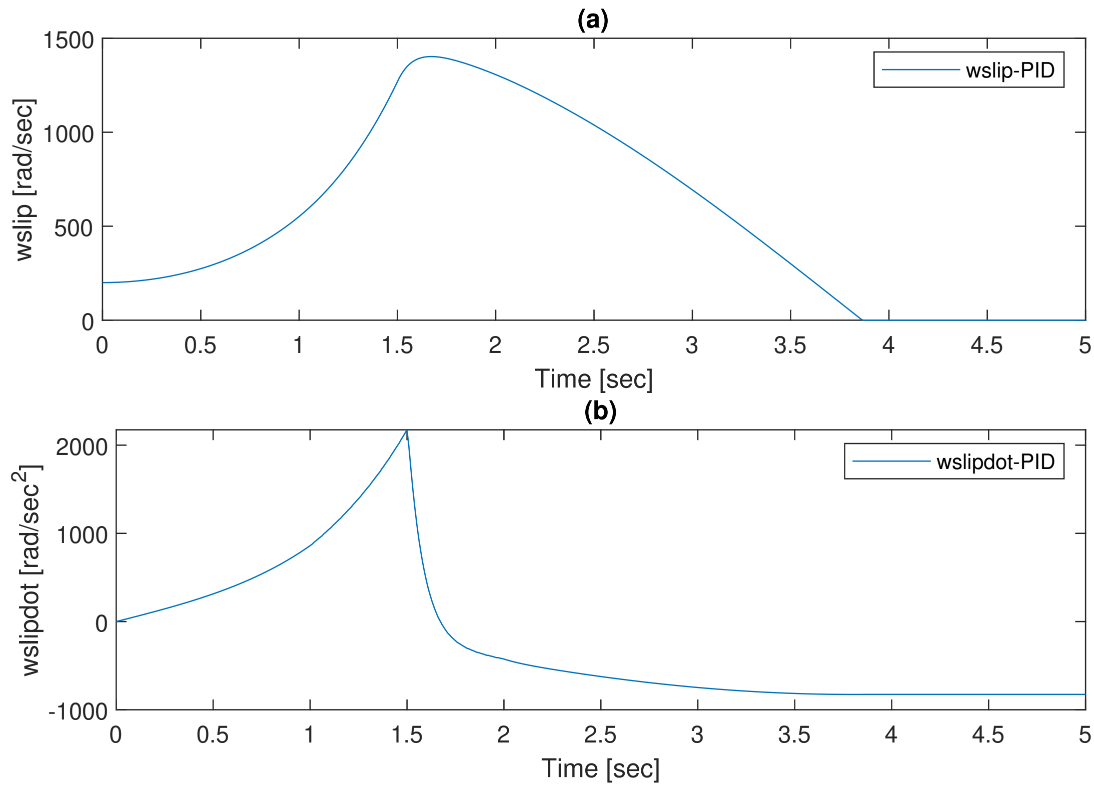

Figure 4.3: System response with PID controller.

to control unstable systems and to solve overshoot problems especially due to time delays in the system [5, 31, 36]. Moreover, the method has advantages to deal with the uncertainty of the systems over classical PID [32].

In PI-PD the control structure, the system has a PD controller in the internal feedback loop to locate the open-loop system poles into proper positions for stability while PI the controller is located on the outer loop of the structure to control the new system created with PD in the inner loop as shown in Fig.4.4 [5, 36].

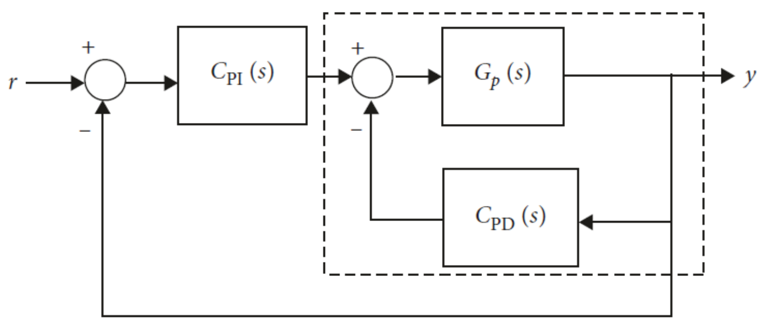

Figure 4.4: PI-PD system structure representation [5].

Thus, PI-PD control is implemented for the system, and the system is simulated again after the parameters of the PI-PD are tuned accordingly. Fig.4.5 shows the differences between the system responses with PID and PI-PD structures.

Fig.4.5 shows that the overshoot on ω_{slip} is solved by PI-PD controller with the expense of $\dot{\omega}_{slip}$. However, it should be noted that this classical control method is only checking one aspect of the system which is the slip speed. Then, methodically, it is not correct to compare the results by checking $\dot{\omega}_{slip}$ behavior. In conclusion, with the classical methods, the system control is simulated with both well-known PID and an improved structure of PI-PD and as expected PI-PD performed better considering ω_{slip} behavior.

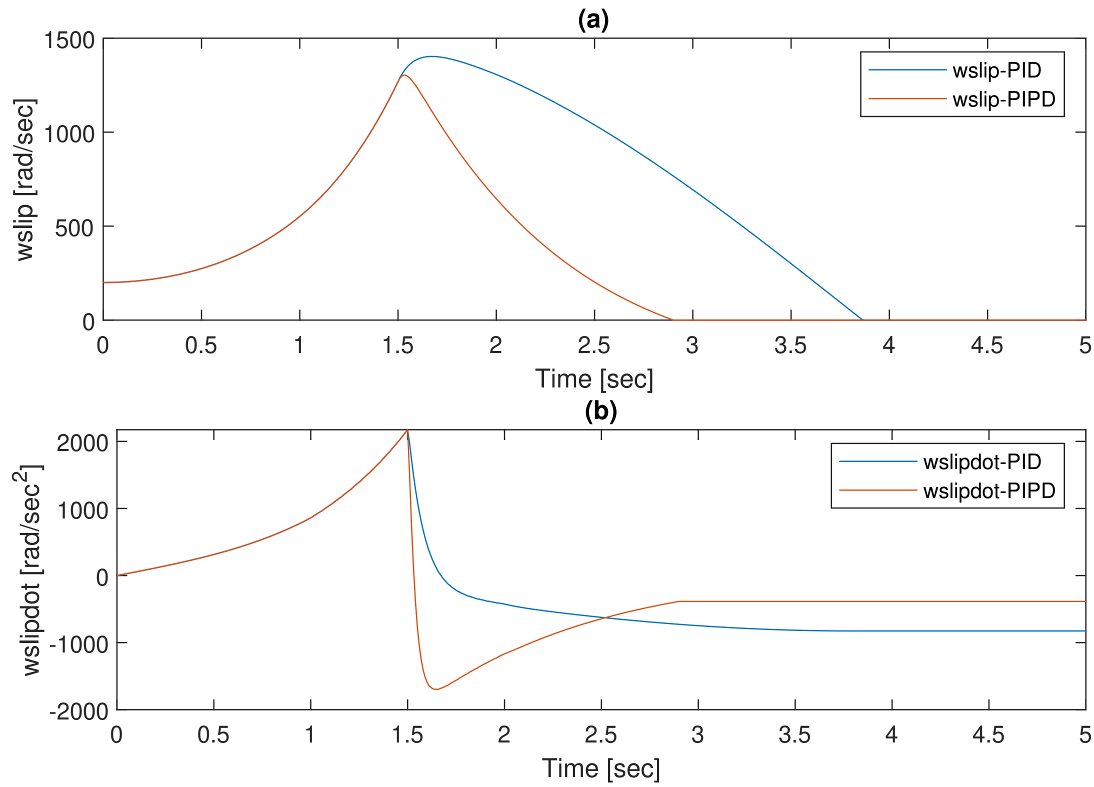

Figure 4.5: System responses with PID and PI-PD controllers, a: ω_{slip}, b: $\dot{\omega}_{slip}$.

4.2 Optimal Control Methods: LQR

In this study, the system is tried to be controlled to make the states of the system zero at the same time. Thus, the control algorithm becomes an optimal control problem. Also, the system is both controllable and observable, so state-space domain control methods (e.g., state feedback) apply to the system. Therefore, the linear quadratic regulator (LQR) method is used as the first method for control since it is one of the most well-known optimization control methods in the literature.

The optimal control strategies aim to calculate control signals which achieve the extremum desired performance criteria (cost function or performance index) under some physical constraints. Being one of the most studied methods, LQR is a unique form of state feedback control approach.

The LQR algorithm aims to calculate controller gain for the state feedback control structure which minimizes the cost function depending on weighted system states and controller output [37–]. The gain is found by LQR algorithm by solving the quadratic cost function as follows:

$$J(u) = \int_0^\infty (x^T Q x + u^T R u) dt \tag{4.5}$$

where Q is the weighting factor matrix for state errors, and R is the weighting factor matrix for regulating the controller signal. The weighting matrix Q determines the importance of the states against each other while the weighting matrix R regulates the aggressiveness of the controller. In other words, the matrix Q is used for punishing the errors of the states with a weighting between them and the matrix R is used for limiting the control signal [38]. For instance, larger R gain will result in a less aggressive controller which will produce a lower control signal and slower system response.

The optimal state feedback controller gain K by LQR is calculated from the equation 4.6.

$$K = R^{-1} B^T P \tag{4.6}$$

where P is calculated from the Algebraic Ricatti Equation as shown in the equation 4.7.

$$A^T P + PA - PBR^{-1}B^T P + Q = 0 \tag{4.7}$$

The system is controlled by different LQR weighting parameters to show the differences in the system in Fig.4.6. According to results, the reduction in R is resulting

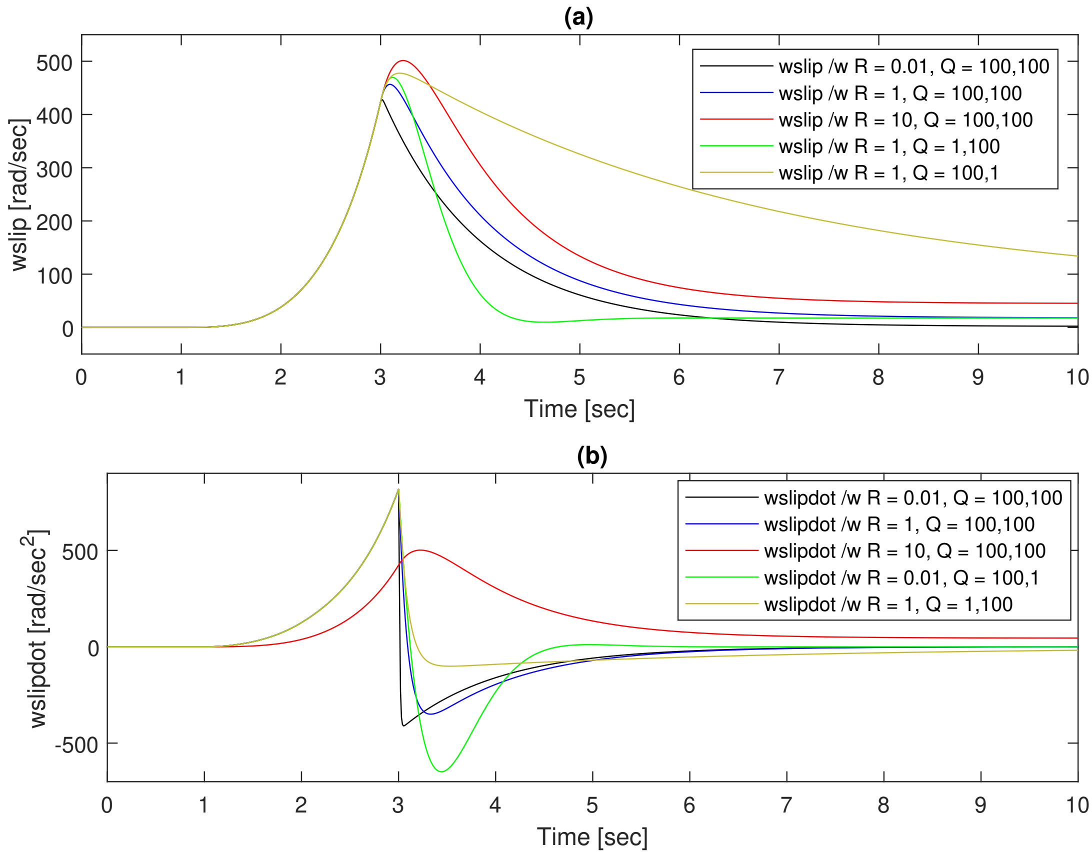

Figure 4.6: System responses with LQR with different weightings, a: ω_{slip}, b: $\dot{\omega}_{slip}$.

in a decrease of controller aggressiveness as expected since it is limiting the control signal. Moreover, the change in the weighting factor for ω_{slip} changes the transient response while also affects the behavior of $\dot{\omega}_{slip}$ (inverse relation). Once $\dot{\omega}_{slip}$ is increased, one of the new system poles(eigenvalues) are placed closer to the origin that slows down the system, also increase in R or ω_{slip} places the poles further away from the origin.

4.2.1 A further approach with LQR:Known disturbances

Until this point, the disturbances (input and output torques) are considered as uncontrolled and unknown aspects. However, for vehicle controls, the torque values of input and output shafts which are engine and transmission input shaft (or EM) torque values are generally known and given to the master controller as real-time signals. They are either measured by sensors or calculated by ECU, MCU, or TCU. Therefore, these torque signals are determined as measured disturbances for the system since they are known aspects of the system in real-time applications.

Therefore, a second approach is implemented considering that the disturbances are known in the system. Then, the effect of disturbances on the system can be removed by manipulating the control signal. Since the inputs of the system are control signal $\dot{P}$, input and output torque changes $\dot{T}_i, \dot{T}_o$, the total system output can be written as in Equation 4.8 where $\tilde{B}$:

$$\tilde{B}_{[2x3]} \begin{bmatrix} U \\ d_1 \\ d_2 \end{bmatrix} = U_{control} + \tilde{B}(2,2) * d_1 + \tilde{B}(2,3) * d_2 \tag{4.8}$$

Then, the control signal can be modified as follows for removing the effects of disturbances.

$$U^* = U - (\tilde{B}(2,2) * d_1 + \tilde{B}(2,3) * d_2) \tag{4.9}$$

After calculating the new control signal equation, the control structure is modified in Simulink environment and the system is simulated. After that, the slip state initial

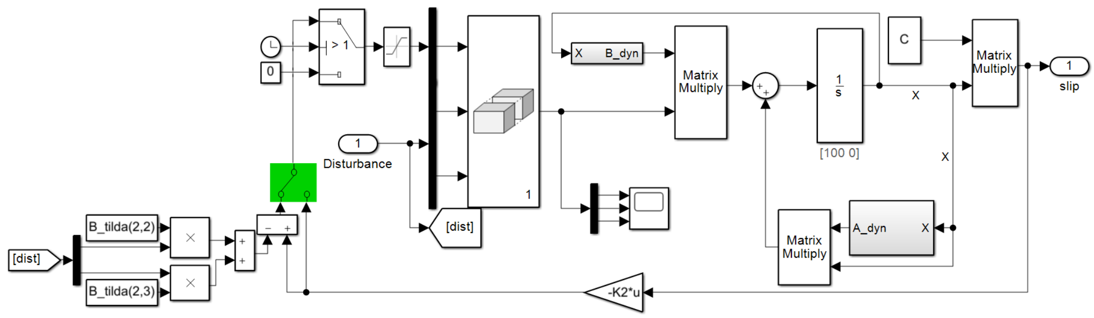

Figure 4.7: LQR structure modification with known disturbances.

value is set to 100 whereas $\dot{T}_o$ is given with a ramp to 20 quantization of 1 when

$\dot{T}_i$ is always zero and the system is simulated and compared with classical LQR as shown in Fig.4.8. According to Fig.4.8 , the second approach in the LQR application is

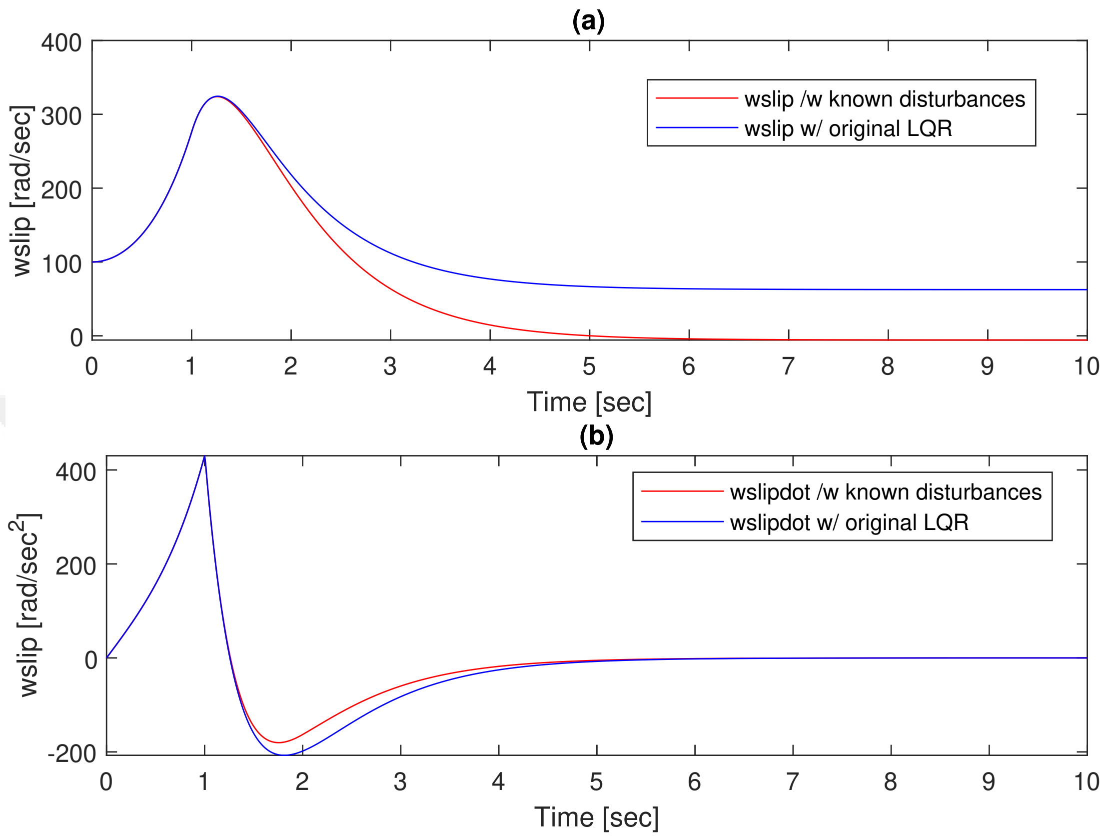

Figure 4.8: System responses with original LQR and known disturbance LQR, a: ω_{slip}, b: $\dot{\omega}_{slip}$.

promising a better performance due to the structure with information on disturbances. It can be noted that, as this approach is modifying the control signal, considering the U^*, if the effect of disturbances increased over the control signal, the effect of the second approach would be more satisfactory.

4.2.2 LQR robustness

After the results with the new approach, the LQR structure is checked against model changes. As mentioned in chapter 3, the dynamic friction coefficient is changing depending on slip speed in the system. For simulations, first, the nominal system controlled, secondly, the dynamic system with changes, finally the dynamic system with more major changes (dynamic model 2) are controlled via a nominal LQR control structure. It has been seen from figure 4.9 the controller cannot control the system if the system dynamics(parameters) is changed more than a threshold. So, the initial LQR controller may not be sufficient to use in all the applications. Thus, the system analysis should be done before controller design and simulations should be performed for determining if this static structure of LQR control is capable of controlling the system. If this approach is not enough, further developments can be done such as a switching algorithm with multiple LQR controllers **which is not part of this study.**

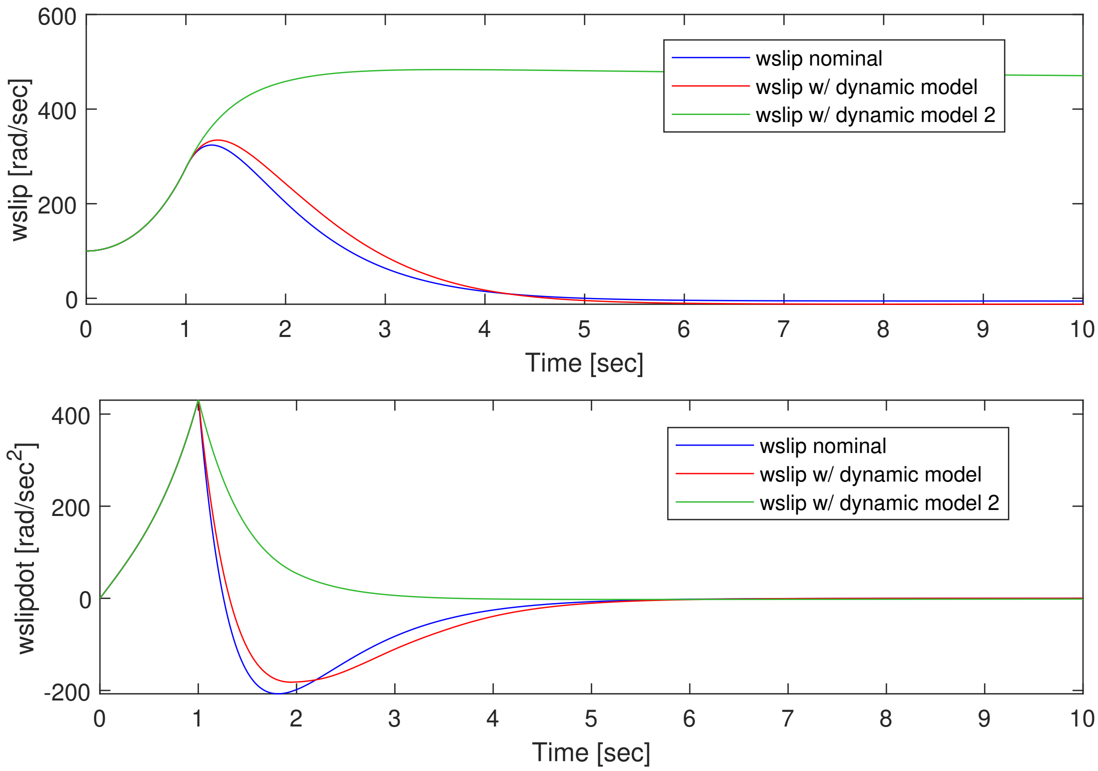

Figure 4.9: Dynamic system responses with LQR.

4.3 Optimal Control Methods: MPC

MPC is also covered in the study due to its popularity in clutch control especially for transmission systems in automotive applications [24, 27]. As described in LQR section the input and output torque signals are determined as measured disturbances also for the MPC controller since in real-time applications they are known aspects of the system.

The system is controlled by an MPC controller by determining the weights of slip speed and slip speed change. MPC uses an algorithm and plant's mathematical model for calculating the future states of the system and calculates an optimized control signal using this information and the knowledge of the measured disturbances in this case. Initially, the weights are determined as 100 for each aspect of slip speed and slip speed change matching with the aim.

4.3.1 MPC algorithm

The main principle of the MPC algorithm is to use a mathematical model of the plant to predict the future steps of the system via receding horizon principle and calculate optimized control signal by solving the quadratic performance index problem. Unlike most methods, MPC is working with a long-range prediction with dynamic structure due to predictions over future horizons at each time step and it has been shown to achieve good performance for the multi-input multi output systems even with dead-time, non-minimum phase, and slow dynamics [14, 40, 41]. Furthermore, there are several proposed approaches to work with MPC for non-linear or linear-time-invariant dynamic systems [15, 40, 42, 43].

Fig.4.10 below shows the generic representation of the MPC methodology at time k. N_p is prediction horizon and N_c is the control horizon. To identify the parameters in more details, prediction horizon N_p represents the number of future samples of the prediction of the system output whereas control horizon represents the number of samples of the optimal control signal will be calculated with the algorithm [6, 40].

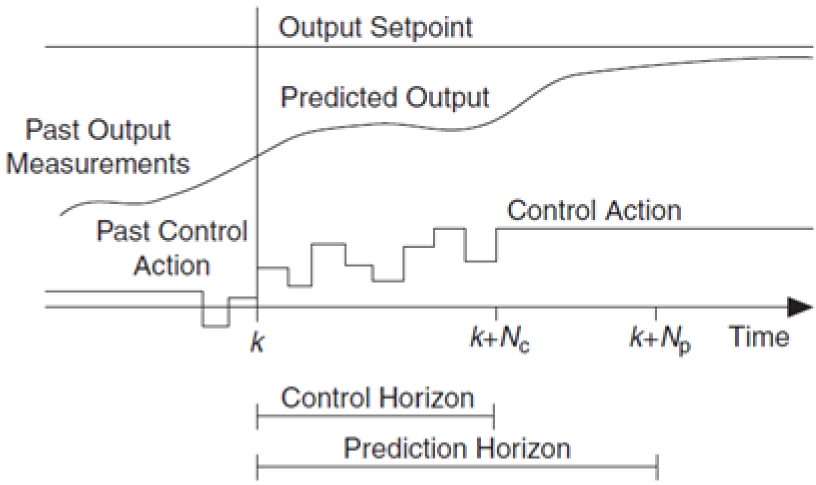

Figure 4.10: MPC Methodology [6].

MPC algorithm can be used with the state-space model which is explained in more detail in chapter 3. This model is used for future estimations. The discrete-time state-space model of the system can be written as in equation 4.10 where A, B, C, D are the state matrices of the system, and d_k is the measurement disturbance [44,45].

$$\begin{aligned} x_{k+1} &= Ax_k + Bu_k \\ y_k &= Cx_k + Du_k + d_k \end{aligned} \tag{4.10}$$

For the sake of simplicity, D and d_k are assumed as zero and the next states are also written below.

$$x_{k+2} = Ax_{k+1} + Bu_{k+1} = A(Ax_k + Bu_k) + Bu_{k+1} = A^2x_k + ABu_k + Bu_{k+1} \tag{4.11}$$

$$y_{k+2} = Cx_{k+1} + Du_k + d_{k+1} = C(Ax_k + Bu_k) \tag{4.12}$$

Thus, the general representation of the equation for n number of predictions can be written as below:

$$\begin{aligned} x_{k+n} &= A^n x_k + A^{n-1}Bu_k + A^{n-2}Bu_{k+1} + \cdots + ABu_{k+n-2} + Bu_{k+n-1} \\ y_{k+n} &= Cx_{k+n} + Du_{k+n} + d_{k+1} = CA^n x_k + CA^{n-1}Bu_k + CA^{n-2}Bu_{k+1} + \\ &\quad \cdots + CABu_{k+n-2} + CBu_{k+n-1} \end{aligned} \tag{4.13}$$

Future states of the system is represented as below for whole prediction horizon (N_p) where $x(k_i + m|k_i)$ is the predicted state at $k+1$ time with the information of system $x(k)$ at k_i where $\Delta u(k) = u(k) - u(k-1)$ [40].

$$\begin{aligned} x(k_i+1|k_i) &= Ax(k_i) + B\Delta u(k_i) \\ x(k_i+2|k_i) &= Ax(k_i+1|k_i) + B\Delta u(k_i+1) \\ &= A^2x(k_i) + AB\Delta u(k_i) + B\Delta u(k_i+1) \\ &\vdots \\ x(k_i+2|k_i) &= A^{N_p}x(k_i+1|k_i) + A^{N_p-1}B\Delta u(k_i) + \\ &\quad A^{N_p-2}B\Delta u(k_i+1) \cdots + A^{N_p-N_c}B\Delta u(k_i+N_c-1) \end{aligned} \tag{4.14}$$

From calculated states for prediction, the output state predictions can be written as below:

$$
\begin{aligned}
y(k_i+1|k_i) &= CAx(k_i)+CB\Delta u(k_i) \\
y(k_i+2|k_i) &= CA^2x(k_i)+CAB\Delta u(k_i)+CB\Delta u(k_i+1) \\
&\;\;\vdots \\
y(k_i+2|k_i) &= CA^{N_p}x(k_i+1|k_i)+CA^{N_p-1}B\Delta u(k_i)+CA^{N_p-2}B\Delta u(k_i+1)+ \\
&\quad \cdots + CA^{N_p-N_c}B\Delta u(k_i+N_c-1)
\end{aligned}
\tag{4.15}
$$

So, future predicted outputs can be reorganized in a compact form for formulation of MPC algorithm by using notations $Y = [y(ki+1|ki)\ y(ki+2|ki)\ y(ki+3|ki)\ldots y(ki+Np|ki)]^T$ and $\Delta U = [\Delta u(k_i)\ \Delta u(k_i+1)\ \Delta u(k_i+2)\ldots \Delta u\,(k_i+N_c-1)]^T$.

$$
Y = Fx(k_i)+\phi\Delta U \tag{4.16}
$$

where

$$
F = \begin{bmatrix} CA \\ CA^2 \\ CA^3 \\ \vdots \\ CA^{N_p} \end{bmatrix}; \Phi = \begin{bmatrix} CB & 0 & 0 & \ldots & 0 \\ CAB & CB & 0 & \ldots & 0 \\ CA^2B & CAB & CB & \ldots & 0 \\ \vdots & & & & \\ CA^{N_p-1}B & CA^{N_p-2}B & CA^{N_p-3}B & \ldots & CA^{N_p-N_c}B \end{bmatrix} \tag{4.17}
$$

After that, the cost function of MPC can be defined in 4.18 similarly with LQR considering R_s as desired outputs of the system where Q and $\overline{R}$ is the controller tuning parameter similar to LQR.

$$
J = (R_s-Y)^T Q(R_s-Y)+\Delta U^T\overline{R}\Delta U \tag{4.18}
$$

Then, the equation 4.18 can be rewritten again using the substations from equation 4.17 for Y and ΔU. After that, the problem becomes a QP optimization problem similar to LQR algorithm and can be solved with QP solvers which is out of scope since MATLAB MPC toolbox is used for the simulations in Simulink in this study.

4.3.2 Simulation results - MPC

Similarly, with LQR, MPC algorithm is implemented with the assumption that the disturbances are known. Firstly, the system is controlled by an MPC controller by determining the weights of ω_{slip} and $\dot{\omega}_{slip}$. Initially, both of the weights are determined as 100 for each system state matching with the aim of study. After that, the weights of the MPC controller are changed in the system and results are plotted as in Fig.4.11. The

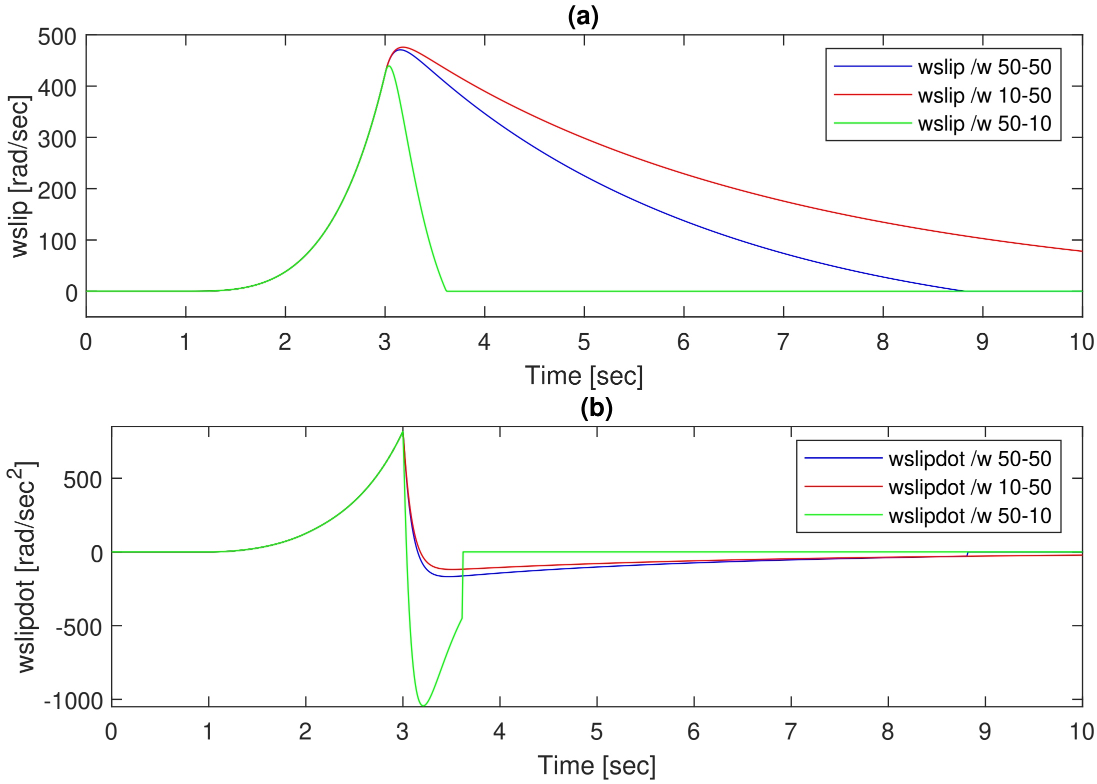

Figure 4.11: : System responses with MPC with different weighting, a: ω_{slip}, b: $\dot{\omega}_{slip}$.

first result is showing when the weights are taken as same which is 50-50. The second line is for weight ratio 10-50. Moreover, the last line shows similarly when the weights are taken 50 and 10 for slip speed and slip speed change, respectively. In simulation, the slip speed becomes negative however at that point, the speed synchronization is finished, and the clutch is locked; also, the control application will be finished, and another operating point is active for the physical system. Thus, the figure only represents the system response until slip speed reaches zero.

As can be seen from Fig.4.11, the increase in $\dot{\omega}_{slip}$ weighting for ω_{slip} weight results in a slowing down in system response which causes more time to finish speed synchronization. However, as it can be seen clearly from "50-10" results, the $\dot{\omega}_{slip}$ is great compared to other applications which will cause a jerk and more feeling to the driver during speed synchronization. These results can be used as a guide to calibrating the weights for real-time applications.

As mentioned in section 3, the real-time system is not static. The kinetic friction coefficient is changing depending on slip speed. For the MPC method, the plant model accuracy is the key aspect of the algorithm. If the mathematical model is not matching with the actual system, the system response might not be as expected according to calculations of the MPC algorithm.

Therefore, a solution is aimed to be implemented using multiple MPCs. This concept can be described as gain scheduled MPC. In this application different MPC controllers are designed to work on different operating points of the system and the switch between these controllers are done during the execution of the application [15].

To simulate this behavior, the state space system is changed during executions by changing the matrix B; element depending on friction coefficient is changed using a look-up table as a function of slip speed as shown in Fig.4.12 and 4.13. After that,

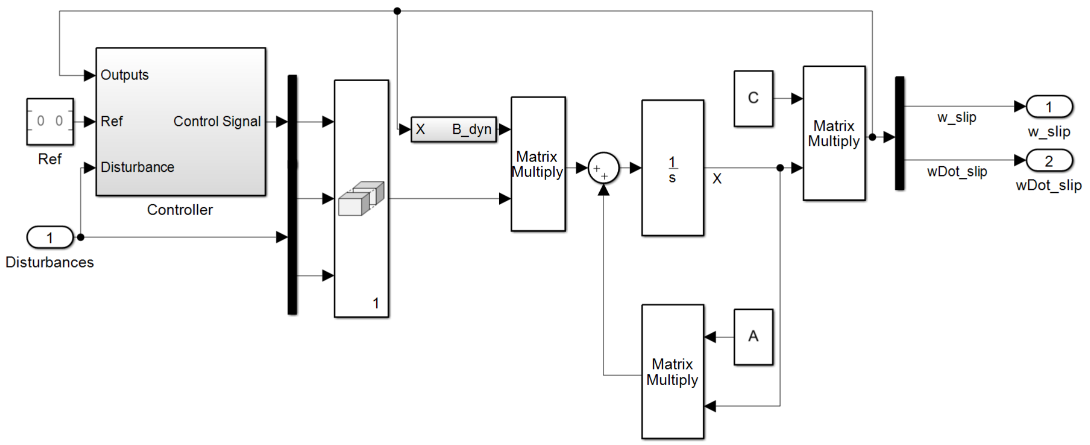

Figure 4.12: Dynamic model of the system depending on slip speed.

multiple MPC controllers are designed by modifying the nominal one by changing the plant models and the multi-MPC structure is built in Simulink as shown in Fig.4.14. After the implementation, the system is simulated and the differences between dynamic system results between with multi-MPC structure and with nominal MPC controller is examined.

For comparing these results, a performance index (PInd) is determined as in equation 4.19. It is used for comparing the results where W_1 and W_2 are weighting factors which are set to 10 and 20, respectively. The performance index punishes the time passes

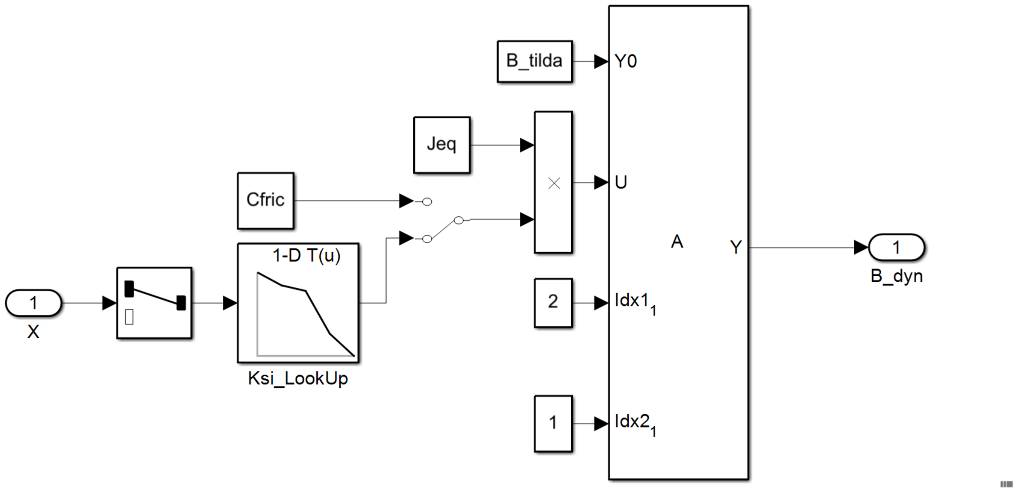

Figure 4.13: Dynamic model aspect of the system depending on slip speed.

to synchronize the speeds with the magnitude of the slip speed. It also considers the slip speed change during the whole process without considering time. In other words, faster synchronization with the least aggressive slip speed change behavior will be the best behavior with the system.

$$PInd = \int_0^{t\omega_{slip}=0} W_1 \ \left|\omega_{slip}\right| t \ dt + \int_0^{t\omega_{slip}=0} W_2 \ \left|\dot{\omega}_{slip}\right| \ dt \tag{4.19}$$

After calculation, results are divided with 10^7 to quantify the results to show a more meaningful number. As shown in Table 4.1, the PInd of the system with nominal

Table 4.1: Performance comparison of nominal-MPC and multi-MPC.

Controller	Performance Index Value
Nominal MPC	52.4974
Multi-MPC	47.8440

MPC is 52.4974 whereas the PInd of the system with multi-MPC is 47.8440 (8.864 % improvement).

Making the study closer to a candidate for a real-time application, the physical limitations of the real system is further considered. Since slip speed change rate cannot be measured directly in most applications, an A Kalman observer is implemented into the system to calculate system outputs and use them as feedback for MPC.

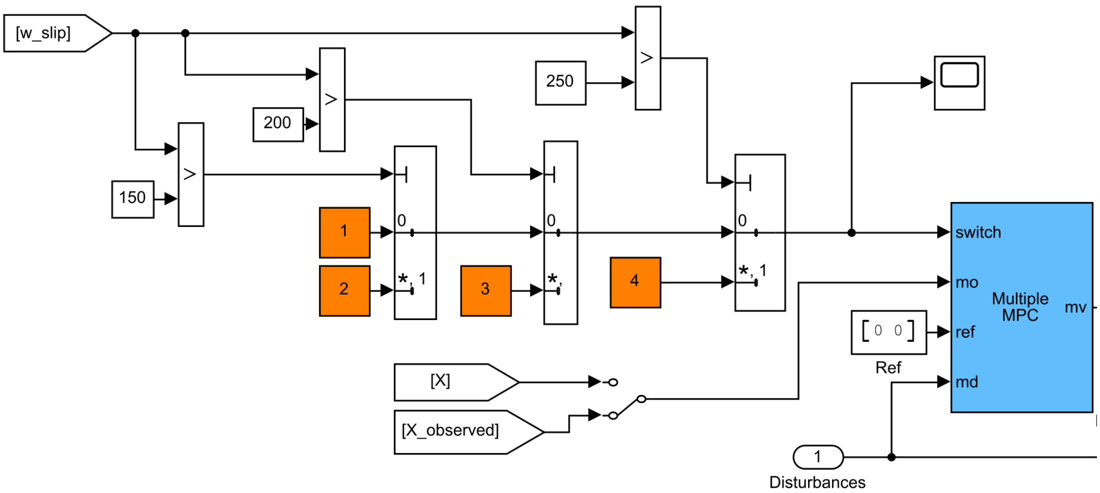

Figure 4.14: Multi-MPC structure in Simulink environment.

4.3.2.1 Feedback for controllers using Kalman filter

The Kalman filter could be described as an estimator algorithm with a prediction correction form using a series of mathematical equations minimization of the error covariance under presumed conditions is the main aim of the estimator by solving an optimization problem. [46]. Kalman filter is one of the most notable subjects in research and applications (especially in the assisted or autonomous navigation) by having a comparably simple structure and its robust nature. Also, the computational advancements for digital control environments in recent years made the Kalman filter is more suitable in real-time applications [46].

An indirect feedback control approach is used for estimation of a system by the Kalman filter. Estimation of the states of the process using measurement data with noise in any sample is the primary aim of the filter Separating the noisy part and meaningful part from sensors is a comprehensive challenge. Also it is the reason why the Kalman system is termed a filter instead of an observer. Measurement update equations and time update equations are two groups of Kalman filter algorithm [46].

The time update part of the Kalman filter is in charge of projecting the current error covariance and state forward (in time) for achieving priori estimates. On the other hand, acquiring an improved posterior estimation by incorporating a new measurement to priori estimation is the main objective of the measurement update part of the filter that makes them responsible for feedback information for the filter. [46]. The set of equations of the Kalman filter are given in equation 4.20.

$$\begin{gathered} x(t) = A(t)x(t) + B(t)u(t) + G(t)w(t) \quad (state\ equation) \\ y(t) = C(t)x(t) + D(t)u(t) + H(t)w(t) + v(t) \quad (measurement\ equation) \end{gathered} \tag{4.20}$$

where $u(t)$ represents the known inputs v is for the white noise of measurement and w represents the processed white noise. The correspondences between measurement and process noises are considered white noise in for the descriptions of $E(vv') = R$, $E(wv') = N$ and $E(ww') = Q$ [47]. N is assumed as zero in this work.

The complete structure of the Kalman filter operation is given in figure 4.15.

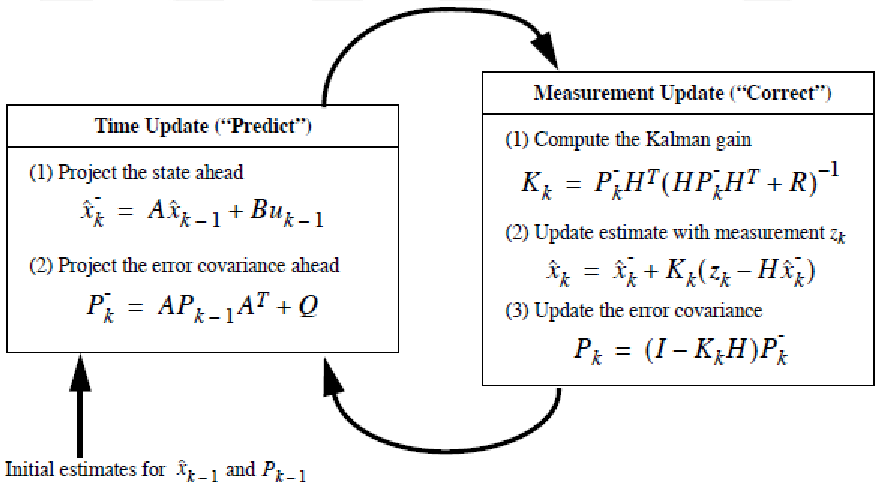

Figure 4.15: Kalman filter complete picture of equations [7]

Moreover, the filter can be applied in MATLAB by determining the mathematical model of the plant, and covariance matrices, R and Q. The Q matrix of covariance can be considered as the weight for the accuracy of the plant model. The R covariance matrix is the measure of the accuracy for the measurement (regarding noises). Both are initially determined as one in this work.

For minimizing the estimation error covariance in the equation 4.21, MATLAB is forming a state estimate of $\hat{x}$.

$$P(t) = E\left[(x-\hat{x})\right]^T \tag{4.21}$$

The Kalman filter problem uses the equations below for finding the optimal solution.

$$L(t) = \left(P(t)C^T(t) + \bar{N}\right) \tag{4.22}$$

$$\hat{\dot{x}}(t) = A(t)\hat{x}(t) + B(t)u(t) + L(t)\left(y(t) - C(t)\hat{x}(t) - D(t)\right) \tag{4.23}$$

L is calculated by the solution of the algebraic Ricatti equation and where

$$\bar{R}(t) = R(t) + H(t)N(t) + N^T(t)H^T(t) + H(t)Q(t)H^T(t) \tag{4.24}$$

$$\bar{N}(t) = G(t)\left(Q(t)H^T(t) + N(t)\right) \tag{4.25}$$

Furthermore the structure for the resulting estimator can be seen as in figure 4.16 It can be concluded from the figure the measurement/output from the real time system y and input u for the system are used for estimating the states and output $\hat{y}\hat{x}$ by the Kalman filter. Using the observer, plant model changes are also considered and given to the

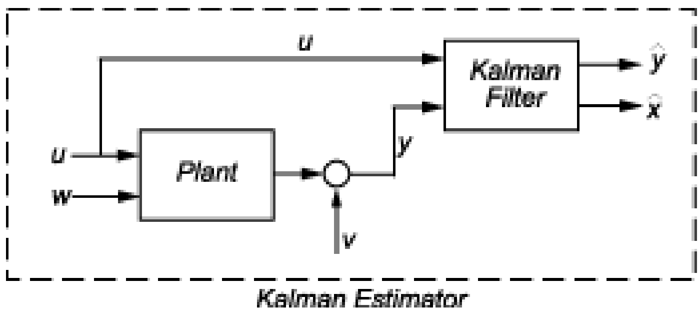

Figure 4.16: Kalman filter structure representation [7].

observer for providing more accurate estimations and Kalman observer is used for state estimation of ω_{slip} and $\dot{\omega}_{slip}$. The Kalman observer simulated under different conditions with different simulations. Since the trivial calibration of Kalman was satisfying and primary focus of the study is not fine-tuning of the observer, spending more effort is considered unnecessary.

4.3.3 Comparison of MPC controllers

After the implementation, the system response differences are compared again as shown in Fig.4.17 and the performance index for multi-MPC with the observer is calculated as in Table 4.2.

Finally, the multi-MPC structure provides the best improvement for the system where multi-MPC structure with Kalman observer still works better than nominal MPC (even with the advantage of nominal MPC structure does not use an observer) in the view of defined performance index but with the expense of $\dot{\omega}_{slip}$.

The difference between multi-MPC and multi-MPC with observer caused by differences in feedback to the system and may not directly relate to an improvement considering ω_{slip} and $\dot{\omega}_{slip}$ together.

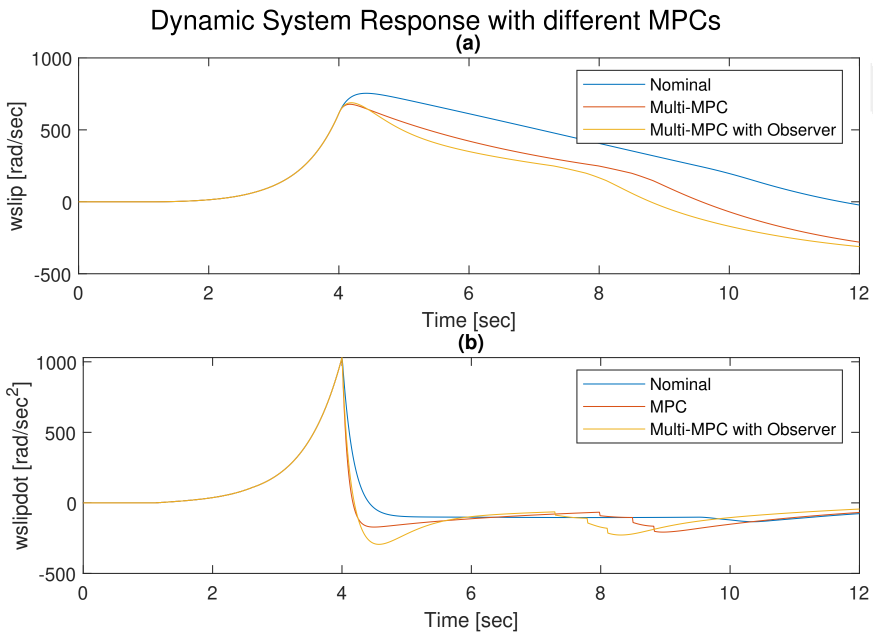

Figure 4.17: Dynamic system response for all MPC controllers.

Table 4.2: Comparison of MPC controllers by performance indexes.

Controller	Performance Index Value
Nominal MPC	52.4974
Multi-MPC	47.8440
Multi-MPC w/observer	48.8717

5. COMPARISON OF ALL CONTROLLERS

The controllers are compared using the performance index described above in one simulation. For comparison, PI-PD, LQR second approach (LQR* in the figure), and multi-MPC structures are used against the dynamic model. As can be seen from Fig.5.1, the controllers are activated after two seconds during the simulation. The results are compared using the performance index mentioned above and controller cost calculated as absolute integral. Then, all results are put to Table 5.1. In Table 5.1,

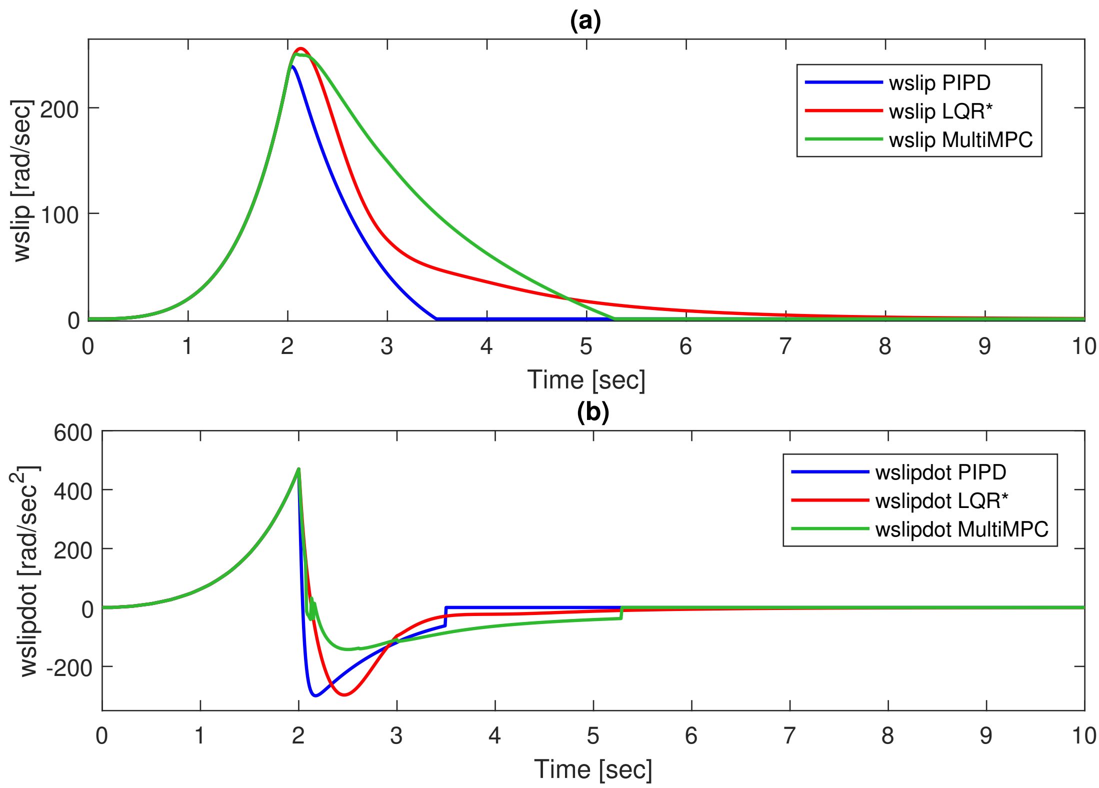

Figure 5.1: Dynamic system response for all controllers, a: ω_{slip}, b: $\dot{\omega}_{slip}$

the mathematical results are shown depending on performance index and controller cost. The cost of the controllers are calculated by absolute integral and the values are quantified such as performance index. In both values, the smaller is better in terms of total performance in terms of the comparison criteria in this study.

Table 5.1: Comparison of all controllers by performance indexes and controller costs.

Controller	Performance Index Value	Controller Cost
PI-PD	198.6133	11.796
LQR*	176.1769	15.7927
Nominal MPC	163.3768	20.8896
Multi-MPC	162.2364	18.8428

It can be deduced that the multi-MPC has provided the best result in this simulation with the highest cost. As expected, the PI-PD response is the best considering only the ω_{slip} since it is suitable and designed for a single input single output part of the system. Even though it has the smallest cost for the control signal; as there is no control structure considering the $\dot{\omega}_{slip}$, then the controller fails in the performance index. LQR* has performed between PI-PD and multi-MPC controller according to the results from table 5.1.

6. CONCLUSIONS AND RECOMMENDATIONS

The purpose of the thesis is to provide a theoretical solution for the practical problem in particular P2 hybrid vehicle systems. The control of the system is studied using classical control methods such as PID and PI-PD; optimal control strategies such as LQR, and model predictive control methods.

First, the modeling of the system is studied using free body diagram principle, and the state-space model of the system is calculated. The expected system response is determined as the system response goes to zero as fast as possible for both outputs, as explained in chapter 4. Then, the system is controlled with the classical PID controller. Having overshoot in the system, a more sophisticated method, the PI-PD controller is used in the system to provide a solution.

After that, the LQR controller is implemented into the system since having a state-space model enables the control engineers to use the optimal control strategies. In the LQR method, the controller gain is calculated once, so the system is static. The parameters of the quadratic problem (Q and R matrices) are essential in this method. After examining the system, it is decided to use two disturbances of the system as measured disturbances. In the automotive field, these quantities will be provided or calculated via sensor information. Thus, another structure is used with LQR using the disturbances as known properties of the system. The robustness of the controllers against model changes is also checked against model changes, which is possible due to the characteristic of the separation clutch system, as explained in detail in chapter 3. According to simulation results, LQR with known disturbances has better system responses against classical LQR. The controller is relatively robust since it can handle system changes unless the change is significant.

After, the system is controlled with the MPC controller using a state-space model. Similarly with LQR, MPC structure used the known disturbances approach. After the simulations with the nominal system, multi-MPC methods are applied for the system against model changes during operation. Additionally, a Kalman filter is implemented to provide a more accurate approach for using real-time applications for system feedback information. The multi-MPC structure has provided the best responses considering the performance index, which described in detail in chapter 4.

Finally, for comparison of the PI-PD controller, LQR with known disturbances and multi-MPC is done. For simulations, the Kalman filter is used for providing feedback information to LQR and MPC. As the results are given, the Multi-MPC controller outperformed the proposed LQR (LQR*) and PI-PD methods. PI-PD can only control the ω_{slip} due to the control structure, whereas the LQR controller is between these two methods.

One of the contributions of this study is considering the system as a compact unit which is separated from other aspects of the powertrain system such as EM and ENG. The system control solutions are considered as independent from EM and ENG. The controllers are only using pressure signal which is a part of the separation clutch unit, unlike most control approaches in the industry where all three elements of EM, ENG, and separation clutch are controlled together. Different control methods over this system are used for proposing a solution which also examined for the responses. Although the control is the primary perspective, the importance of dynamic model changes and feedback information for the system have been intensified.

The study is open for further improvements in terms of fine-tuning of parameters and introducing more complex methods. Since the LQR algorithm tries to ensure that ω_{slip} and $\dot{\omega}_{slip}$ go to zero as soon as possible, further tuning on LQR weight parameters results in better responses. Similarly, it should be noted that the PI-PD results are the results after trivial optimization tuning during this paper. There might be better results by further investigation and tuning of the parameters. Furthermore, different structures for proposed controllers can be introduced to the system as future works such as multiple gains for LQR against model changes and a different approach to PI-PD by taking $\dot{\omega}_{slip}$ into account.

REFERENCES

[1] **Salmasi, F.R.** (2007). Control Strategies for Hybrid Electric Vehicles : Evolution , Classification , Comparison , and Future Trends, *IEEE Transactions on Vehicular Technology*, *56*(5), 2393–2404.

[2] **Wu, G.**, **Zhang, X. and Dong, Z.** (2015). Powertrain architectures of electri fi ed vehicles : Review , classi fi cation and comparison, *Journal of the Franklin Institute*, *352*, 425–448.

[3] **Nüesch, Tobias Cerofolini, Alberto Mancini, Giorgio Cavina, Nicolo Onder, Christopher and Guzzella, L.** (2014). Equivalent Consumption Minimization Strategy for the Control of Real Driving NO Emissions of a Diesel Hybrid Electric Vehicle, *Energies*, *7*, 3148–3178.

[4] "Mathworks - Disk Friction Clutch", `https://ch.mathworks.com/help/physmod/sdl/ref/diskfrictionclutch.html`, accessed: 2020.

[5] **Zheng, M.**, **Huang, T. and Zhang, G.** (2019). A New Design Method for PI-PD Control of Unstable Fractional-Order System with Time Delay, *Complexity*, *2019*, 1–12.

[6] **Derouiche, M.L.**, **Bouallègue, S.**, **Haggège, J. and Sandou, G.** (2016). LabVIEW perturbed particle swarm optimization based approach for model predictive control tuning, *IFAC-PapersOnLine*, *49*(5), 353–358.

[7] "Mathworks-Kalman", `https://www.mathworks.com/help/control/ref/ss.kalman.html`, accessed: 2020.

[8] **Enang, W. and Bannister, C.** (2017). Modelling and control of hybrid electric vehicles (A comprehensive review), *Renewable and Sustainable Energy Reviews*, *74*, 1210–1239, `http://dx.doi.org/10.1016/j.rser.2017.01.075`.

[9] **Hannan, M.A.**, **Azidin, F.A. and Mohamed, A.** (2014). Hybrid electric vehicles and their challenges : A review, *Renewable and Sustainable Energy Reviews*, *29*, 135–150, `http://dx.doi.org/10.1016/j.rser.2013.08.097`.

[10] **Sulaiman, N.**, **Hannan, M.A.**, **Mohamed, A.**, **Majlan, E.H. and Daud, W.R.W.** (2015). A review on energy management system for fuel cell hybrid electric vehicle : Issues and challenges, *Renewable and Sustainable*

Energy Reviews, *52*, 802–814, http://dx.doi.org/10.1016/j.rser.2015.07.132.

[11] **Sireesha Tamada , Debraj BhattacharjeeDan, P.K.** (2020). Review on automatic transmission control in electric and non-electric automotive powertrain, *Int. J. Vehicle Performance*, *6*(1), 98–128.

[12] **Ding, Jingang Jiao, X.** (2020). A Novel Control Method of Clutch During Mode Transition of Single-Shaft Parallel Hybrid, *Electronics*, *9*(54), 1–16.

[13] **Garofalo, F.**, **Glielmo, L. and Iannelli, L.** (2002). Optimal Tracking for Automotive Dry Clutch, *IFAC Proceedings Volumes*, volume 35, IFAC, pp.367–372, http://dx.doi.org/10.3182/20020721-6-ES-1901.01529.

[14] **Bemporad, A.**, **Borrelli, F.**, **Glielmo, L. and Vasca, F.** (2001). Hybrid Control of Dry Clutch Engagement, *European Control Conference*, pp.635–639.

[15] "Mathworks - Multiple MPC Controllers", https://ch.mathworks.com/help/mpc/ref/multiplempccontrollers.html, accessed: 2020.

[16] **He, X.**, **Parten, M. and Maxwell, T.** (2005). Energy Management Strategies for a Hybrid Electric Vehicle, *IEEE Vehicle Power and Propulsion Conference*, pp.536–540.

[17] **Hu, X.**, **Murgovski, N.**, **Johannesson, L. and Egardt, B.** (2013). Energy efficiency analysis of a series plug-in hybrid electric bus with different energy management strategies and battery sizes, *Applied Energy*, *111*, 1001–1009, http://dx.doi.org/10.1016/j.apenergy.2013.06.056.

[18] **Pisu, P. and Rizzoni, G.** (2007). A Comparative Study Of Supervisory Control Strategies for Hybrid Electric Vehicles, *IEEE Transactions on Control System Technology*, *15*(3), 506–518.

[19] **Chan, C.C.** (2007). The state of the art of electric, hybrid, and fuel cell vehicles, *Proceedings of the IEEE*, *95*, 704–718.

[20] **Xiong, W.**, **Zhang, Y. and Yin, C.** (2009). Optimal energy management for a series – parallel hybrid electric bus, *Energy Conversion and Management*, *50*(7), 1730–1738, http://dx.doi.org/10.1016/j.enconman.2009.03.015.

[21] **Maggetto, P.G. and Mierlo, V.** (2010). Electric and Electric Hybrid Vehicle Technology: A Survey, *IEE Seminar on Electric, Hybrid and Fuel Cell Vehicles*, pp.1–11.

[22] **Negarestani, S.**, **Ghahnavieh, A.R. and Mobarakeh, A.S.** (2012). A Study of The Reliability of Various Types of The Electric Vehicles, *IEEE International Electric Vehicle Conference*, pp.1–6.

[23] **Liu, J.**, **Peng, H. and Filipi, Z.** (2005). Modeling and Analysis of the Toyota Hybrid System, *International Conference on Advanced Intelligent Mechatronics*, pp.24–28.

[24] **Heijden, A.C.V.D.**, **Serrarens, A.F.A.**, **Camlibel, M.K.**, **Nijmeijer, H.**, **Serrarens, A.F.A.**, **Camlibel, M.K. and Nijmeijer, H.** (2007). Hybrid optimal control of dry clutch engagement Hybrid optimal control of dry clutch engagement, *International Journal of Control*, *80*(11), 1717–1728.

[25] “Mathworks - Fundamental clutch”, `https://ch.mathworks.com/help/physmod/sdl/ref/fundamentalfrictionclutch.html`, accessed: 2020.

[26] "Mathworks-Disc Clutch", `https://ch.mathworks.com/help/autoblks/ref/discclutch.html`, accessed: 2020.

[27] **Pisaturo, M.**, **Cirrincione, M.**, **Member, S. and Senatore, A.** (2015). Multiple Constrained MPC Design for Automotive Dry Clutch Engagement, *IEEE/ASME Transactions on Mechatonics*, *20*(1), 469–480.

[28] **Ogata, K.** (2010). *Modern Control Engineering*, Prentice Hall, Upper Saddle River, NJ, vol. 5 edition.

[29] **Lawrence, R.L.W.I. and A., D.**, (2007). Observability, Linear State-Space Control Systems, John Wiley & Sons, pp.149–184.

[30] **Kocur, M.**, **Kozak, S. and Dvorscak, B.** (2014). Design and Implementation of FPGA - digital based PID controller, *Proceedings of the 2014 15th International Carpathian Control Conference (ICCC)*, pp.233–236.

[31] **Dincel, E. and Söylemez, M.T.** (2018). Digital PI-PD controller design for arbitrary order systems : Dominant pole placement approach, *ISA Transactions*, 1–13, `https://doi.org/10.1016/j.isatra.2018.04.009`.

[32] **Ali, H.** (2016). Robust PI-PD Controller Design for Systems with Parametric Uncertainties, *Eng. &Tech.Journal*, *34*(Part A,No.11), 2167–2173.

[33] **Munro, N. and Söylemez, M.** (2000). Fast Calculation of Stabilizing PID Controllers for Uncertain Parameter Systems, *IFAC Proceedings Volumes*, *33*, 549–554.

[34] **Wang, Q.G.**, **Zhang, Z.**, **Astrom, K.J.**, **Zhang, Y. and Zhang, Y.** (2008). Guaranteed Dominant Pole Placement with PID Controllers, *IFAC Proceedings Volumes*, *41*(2), 5842 – 5845, `http://www.sciencedirect.com/science/article/pii/S1474667016398779`, 17th IFAC World Congress.

[35] **Munro, N.** (2001). The systematic design of PID controllers using Nyquist stabiliy, *2001 European Control Conference (ECC)*, pp.528–533.

[36] **Kaya, I. and Atherton, D.P.** (2006). Simple analytical rules for PI-PD controllers to tune integrating and unstable processes, *International Control Conference*.

[37] **Jr, L.A.M.**, **Valle, R.L.**, **Ferreira, A.A.**, **Barbosa, P.G. and Montagner, V.F.** (2016). A Lqr Design With Rejection Of Disturbances And Robustness To Load Variations Applied To A Buck Converter, *Eletrônica de Potência*, *21*(1), 7–15.

[38] **Durmaz, B.E.**, **Berkan, K.**, **Mutlu, I. and Turan, M.** (2017). Implementation and Comparison of LQR-MPC on Active Suspension System, *10th International Conference on Electrical and Electronics Engineering (ELECO)*, pp.828–835.

[39] **Almobaied, M.**, **Eksin, I. and Guzelkaya, M.** (2016). Design of lqr controller with big bang-big crunch optimization algorithm based on time domain criteria, *2016 24th Mediterranean Conference on Control and Automation (MED)*, IEEE, pp.1192–1197.

[40] **Wang, L.** (2009). *Model Predictive Control System Design and Implementation Usng MATLAB*, Springer UK.

[41] **Morari, M. and Lee], J.H.** (1999). Model predictive control: past, present and future, *Computers & Chemical Engineering*, *23*(4), 667 – 682, `http://www.sciencedirect.com/science/article/pii/S0098135498003019`.

[42] **Mo, H. and Farid, G.** (2019). Nonlinear and Adaptive Intelligent Control Techniques for Quadrotor UAV- A Survey, *Asian Journal of Control*, *21*(2), 989–1008.

[43] **Franco, A.** (2019). Short-term Path Planning with Multiple Moving Obstacle Avoidance based on Adaptive MPC, *2019 IEEE International Conference on Autonomous Robot Systems and Competitions (ICARSC)*, 1–7.

[44] **Bemporad, A.**, **Morari, M. and Ricker, N.** (2000). The MPC simulink library, *Automatic Control Laboratory Physikstrasse*, *3*, 8092.

[45] **Kendir, F.** (2018). Forward and Inverse Fuzzy Based Model Predictive Control of a Turbocharged Diesel Engine with High-Pressuere Exhaust Gas Recirculation System, *Ph.D. thesis*, Istanbul Technical University.

[46] **Bishop, G.**, **Welch, G.** *et al.* (2001). An introduction to the kalman filter, *Proc of SIGGRAPH, Course*, *8*(27599-23175), 41.

[47] **Deshpande, A.S.** (2017). Bridging a Gap in Applied Kalman Filtering: Estimating Outputs When Measurements Are Correlated with the Process Noise [Focus on Education], *IEEE Control Systems Magazine*, *37*(3), 87–93.

CURRICULUM VITAE

Name Surname:
Berkan KAÇMAZ
Place and Date of Birth:
07.07.1994 - BANDIRMA
E-Mail:
kacmazb@itu.edu.tr

EDUCATION:

- **B.Sc.:** 2017, Istanbul Technical University, Control and Automation Engineering, Electric Electronic Department

PROFESSIONAL EXPERIENCE AND REWARDS:

- 2017- Ongoing AVL Turkey Research and Engineering.

PUBLICATIONS:

- **Durmaz, B., Kaçmaz B.,Mutlu I., Soylemez, M., 2017. Implementation and Comparison of LQR-MPC on Active Suspension System,** *ELECO,* 48(17), 5195-5220.

- **Kaçmaz B.,Durmaz, B.,Mutlu İ., Söylemez, M., 2017. Aktif Süspansiyon Sistemi: Farklı Kontrol Yöntemlerinin Uygulanması,** *Otomatik Kontrol Ulusal Toplantısı TOK'17*